

HYDROXYL ROTATIONAL TEMPERATURES  
IN THE AIRGLOW

A Thesis

Submitted to the Faculty of Graduate Studies  
in Partial Fulfilment of the Requirements  
for the Degree of  
Master of Science  
in the Department of Physics  
University of Saskatchewan

by

David Conway Nicholls  
Saskatoon, Saskatchewan  
February, 1971

The author claims copyright. Use shall not be made of the  
material contained herein without proper acknowledgement.

UNIVERSITY OF SASKATCHEWAN

College of Graduate Studies

Saskatoon

CERTIFICATION OF THESIS WORK

We, the undersigned, certify that DAVID CONWAY NICHOLLS

(full name)

B.Sc. (HONOURS)  
(degrees)

candidate for the degree of MASTER OF SCIENCE

has presented his thesis with the following title: "HYDROXYL ROTATIONAL  
TEMPERATURES IN THE AIRGLOW"

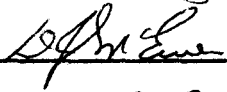
(as it appears on title page of thesis)

that the thesis is acceptable in form and content, and that a satisfactory  
knowledge of the field covered by the thesis was demonstrated by the candidate  
through an oral examination held on FRIDAY, FEBRUARY 12, 1971.

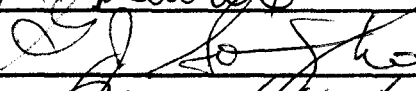
External Examiner 

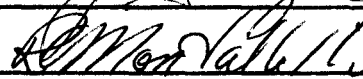
Professor of Chemistry

Internal Examiners 

  
Edward J. Penally

  
H. A. Rundle

  
J. L. G. Ho

  
W. M. V. H.

UNIVERSITY OF SASKATCHEWAN

PERMISSION TO USE POSTGRADUATE THESES

Title of Thesis "HYDROXYL ROTATIONAL TEMPERATURES IN THE AIRGLOW"

Name of Author DAVID CONWAY NICHOLLS

Department or College PHYSICS

Degree MASTER OF SCIENCE

In presenting this thesis in partial fulfilment of the requirements for a postgraduate degree from the University of Saskatchewan, I agree that the Libraries of this University may make it freely available for inspection. I further agree that permission for extensive copying of this thesis for scholarly purposes may be granted by the professor or professors who supervised my thesis work or, in their absence, by the Head of the Department or the Dean of the College in which my thesis work was done. It is understood that any copying or publication or use of this thesis or parts thereof for financial gain shall not be allowed without my written permission. It is also understood that due recognition shall be given to me and to the University of Saskatchewan in any scholarly use which may be made of any material in my thesis.

Signature

*David C Nicholls*

Address

*Kelsey Hwy  
U7S Saskatoon  
Sask*

Date February 12, 1971.

## ACKNOWLEDGEMENTS

It gives me considerable satisfaction to acknowledge the assistance afforded me during my work on this project. In particular I would like to thank Dr. E. J. Llewellyn for his capable supervision of the project, and for many interesting and fruitful discussions. I also wish to thank Dr. A. W. Harrison for supplying the observational data on which this project has been based. Also I would like to thank Dr. B. W. Currie and Dr. R. J. Skinner for valuable advice during the writing of this thesis. I am indebted for the typing of the thesis to Miss Beverley Konsmo, without whose generous help the work would have experienced considerable delays.

I would like to acknowledge financial support from C.A.R.D.E. contracts awarded to the University of Saskatchewan.

D. C. Nicholls

## ABSTRACT

Nightglow spectra of the OH Meinel bands have been analysed to determine the rotational temperature. It has been found that the rotational temperatures determined from different rotational lines in a single band are not constant but increase with increasing rotational quantum number. A deviation from isothermal rotational temperatures for excited molecules in rotational equilibrium is caused by the variation of kinetic temperature in the OH emission region, but is much less than that observed. It has been concluded that non-equilibrium processes are important. A rotational relaxation model has been proposed to describe the spectrum emitted by molecules that are not in rotational equilibrium. The model was used to calculate the OH nightglow spectrum for bands originating from the eighth and ninth vibrational levels. The calculated rotational temperatures are in good agreement with those derived from observed spectra.

The effects of vibrational relaxation in the excited OH molecules have been considered qualitatively and are in agreement with the observed behaviour of the measured intensities and rotational temperatures.

It is suggested that the application of the relaxation model to other airglow emissions may give new information on atmospheric processes.

## TABLE OF CONTENTS

	Page
Title Page .....	i
Acknowledgements .....	iii
Abstract .....	iv
Table of Contents .....	v
List of Figures .....	x
List of Tables .....	xi

### Chapter

I. INTRODUCTION .....	1
1.1 Temperature Determination in the Atmosphere .....	1
1.2 OH Airglow Emissions .....	2
1.3 Summary of Presentation .....	3
II. SPECTROSCOPY AND ROTATIONAL TEMPERATURES .....	5
2.1 Introduction .....	5
2.2 Energy Levels .....	5
2.2.1 Angular momenta .....	5
2.2.2 Coupling of angular momenta .....	6
2.2.3 Coupling intermediate between case (a) and case (b) .....	8
2.2.4 Vibrational energy levels .....	10
2.2.5 Total energy .....	11
2.3 Diatomic Spectra .....	12
2.3.1 Transition selection rules .....	12
2.3.2 Vibration-rotation spectra .....	12

## TABLE OF CONTENTS (continued)

Chapter		Page
II.	2.3.3 Vibration-rotation spectrum of OH .....	14
	2.3.4 Intensity of emission lines .....	15
	2.3.5 Line strength factors .....	18
	2.3.6 Transition probabilities .....	21
	2.4 The Determination of Temperature from Rotational Spectra .....	21
	2.4.1 Graphical method .....	21
	2.4.2 Relative branch intensity method .	23
	2.4.3 Spin doublet temperature .....	23
	2.4.4 Comparison of spectra .....	24
	2.5 Survey of Previous Work .....	24
III.	NON-ISOTHERMAL BEHAVIOUR IN OH AIRGLOW ROTATIONAL TEMPERATURES. 1. EQUILIBRIUM CONDITIONS .....	27
	3.1 Introduction .....	27
	3.2 Profile Weighted Spectral Temperatures ..	27
	3.2.1 Observed OH emission height profiles .....	27
	3.2.2 Calculated rotational spectra ....	30
	3.3 Atmospheric Profiles from Ground Based Measurements .....	36
	3.4 Vibration Rotation Interaction and Line Strengths .....	37
	3.4.1 Introduction .....	37
	3.4.2 Analysis for estimated interaction factors .....	38
	3.4.3 Other uncertainties in the line strengths .....	40

## TABLE OF CONTENTS (continued)

Chapter	Page
III. 3.5 The Effect of Failure to Resolve the Spin Doublet Components .....	42
3.6 The Effect of Background on Rotational Temperature Determination .....	44
3.7 Self-absorption .....	45
3.8 Instrument Effects .....	48
3.8.1 Step-scanning spectrometer .....	48
3.8.2 Photographic plates .....	50
3.9 Discussion .....	51
IV. NON-ISOTHERMAL BEHAVIOUR IN OH AIRGLOW ROTATIONAL TEMPERATURES. 2. NON- EQUILIBRIUM CONDITIONS .....	52
4.1 Introduction .....	52
4.2 Origin of the Initial Populations .....	54
4.3 The Effect of Transitions on Rotational Population Distribution .....	55
4.3.1 Theoretical considerations .....	55
4.3.2 The variation of the transition effect for different bands ....	57
4.3.3 Quantitative calculation of the transition effect .....	58
4.4 Partial Thermalization in Non-Equilibrium Populations .....	59
4.4.1 Introduction .....	59
4.4.2 Relaxation processes .....	61
4.4.3 Simple relaxation with radiative loss mechanisms .....	63
4.4.4 Discussion of the simple model ..	65



## TABLE OF CONTENTS (continued)

Chapter	Page
IV. 4.5 Weak Interaction Relaxation Theory .....	66
4.5.1 Introduction .....	66
4.5.2 Rotational relaxation .....	66
4.5.3 Solution of the relaxation equation .....	71
4.5.4 Radiative relaxation .....	73
4.6 Applicability of Weak Interaction Theory to Rotational Relaxation Processes ...	77
V. APPLICATION OF RELAXATION PROCESSES TO THE AIRGLOW EMISSIONS .....	80
5.1 Excitation Mechanisms for the OH Airglow .....	80
5.1.1 Introduction .....	80
5.1.2 Hydrogen-Ozone reaction .....	80
5.1.3 Rotational level populations ....	82
5.1.4 Spin doublet level populations ..	83
5.1.5 Initial populations in airglow calculations .....	85
5.2 Calculation of the OH Airglow Spectrum by the Weak Interaction Relaxation Process .....	86
5.2.1 Calculation of ground based spectra .....	86
5.2.2 Numerical results .....	87
5.2.3 Discussion .....	95
5.3 The Role of Vibrational Relaxation .....	96
5.3.1 Introduction .....	96
5.3.2 Theory .....	97

## TABLE OF CONTENTS (continued)

Chapter	Page
V.        5.3.3    Temperature dependence and band intensities .....	98
5.3.4    Comparison with observations ....	99
VI.    SUMMARY AND CONCLUSIONS .....	103
6.1    The Present Work .....	103
6.2    Suggestions for Future Work .....	106
6.2.1    OH emissions .....	106
6.2.2    Application to other emissions ..	108
LIST OF REFERENCES .....	112

## LIST OF FIGURES

Figure	Page
2.1 OH (5-2) band spectrum calculated for a spectrometer slit-width of 27A, at a temperature $T = 180^{\circ}\text{K}$ .....	16
3.1 Measured OH emission height profiles .....	29
3.2 Atmospheric temperature profile, summer $45^{\circ}$ latitude (United States Standard Atmosphere tables, 1966) .....	31
3.3 Rotational temperature graph for the P1 lines, (8-4) band, calculated for the Packer (1961) emission height profile .....	33
3.4 Rotational temperature graphs for observed OH (8-3) and (8-4) band spectra .....	49
4.1 Rotational relaxation in a non-radiating population. (Time units in terms of $1/\nu_{\text{coll}}$ .) .....	74
4.2 Effective Population distribution for different ratios of collision frequency and transition probability .....	76
5.1 Comparison of rotational temperature graphs for theory and observations .....	94

## LIST OF TABLES

Table	Page
2.1 Selection rules for electric dipole transitions ..	13
2.2 Line strength values .....	20
2.3 Relative transition probabilities for OH, $A_{v',v''}$ ..	22
3.1 OH nightglow emission profile measurements .....	28
3.2 Comparison of theoretical and observational rotational temperatures .....	35
3.3 The effect of errors in line strength values. (Equilibrium temperature 200°K) .....	41
3.4 The effect of using P1 line strengths in the analysis of unresolved P line spin doublets ....	43
3.5 The effect of background on rotational temperatures (Equilibrium temperature 200°K) .....	46
4.1 Collision frequency as a function of height (Calculated from 1966 United States Standard Atmosphere Data) .....	53
4.2 Transition effect, (7-3) band. (Rotational population temperatures of lower state, for a range of upper state equilibrium temperature $T_{EQ}$ (°K).) .....	60
5.1 OH energy levels near the reaction energy, (26969 $\text{cm}^{-1}$ ) .....	84
5.2 Effective rotational populations of ninth vibrational level as a function of height .....	88
5.3 Rotational temperatures ( $T_{ROT}$ ) of effective emitting population, ninth vibrational level ...	89
5.4 Effective rotational populations of eighth vibrational level as a function of height .....	92
5.5 Rotational temperatures ( $T_{ROT}$ ) of effective emitting population, eighth vibrational level ..	93

## CHAPTER I

### INTRODUCTION

#### 1.1 Temperature Determination in the Atmosphere

A knowledge of the atmospheric temperature profile and its variation is necessary for an understanding of many atmospheric phenomena. Direct sounding of the upper atmosphere is both expensive and complicated so that synoptic measurements of the type made for the lower atmosphere are not in general attempted. Indirect determination of kinetic temperatures in the upper atmosphere is possible from pressure and density measurements obtained with rockets and satellites, and from ground-based spectroscopic measurements of the aurora and airglow. If the heights of the aurora or airglow emissions are known, spectroscopic methods can provide an inexpensive method for determining the kinetic temperature profile in the atmosphere.

Temperatures derived from spectroscopic measurements are of three general types; Doppler, or line width temperatures, vibrational temperatures, and rotational temperatures. The nature of the temperature information obtained from molecular vibrational and rotational spectra will be determined by the approximation to thermal equilibrium of the excited molecules. If the molecules are in rotational or vibrational equilibrium, the rotational or vibrational temperature determined from the emission spectrum will be equal to the kinetic temperature at the emission height. If equilibrium has not been established

in the molecular rotational or vibrational level populations at the time the molecules radiate, the derived temperature is related to the excitation temperature, and is not a measure of the kinetic temperature. Spectroscopic temperatures determined from allowed electric dipole transitions may be either excitation temperatures or kinetic temperatures. For these transitions, the upper state has, in general, a very short lifetime ( $\sim 10^{-7}$  sec.) and the excited molecules will therefore have a small probability of collisional redistribution of the rotational and vibrational populations. If the emissions arise from forbidden transitions, the lifetime of the upper state is long ( $> .1$  sec.) and it is to be expected that the emitting populations will be in thermal equilibrium.

For most atmospheric molecules, collisional redistribution is much more efficient for the rotational population than for the vibrational population (Herman and Shuler, 1958). Therefore, it is possible that for some excited molecular species rotational equilibrium is established before emission, while vibrational equilibrium is not. For these molecules, the rotational temperatures will indicate the ambient kinetic temperature, while the vibrational temperatures will give information on the excitation mechanism of the vibrational population.

## 1.2 OH Airglow Emissions

The OH airglow emissions have been the subject of extensive investigation since their identification by Meinel (1950). These emissions arise from transitions between the

vibrational and rotational energy levels in the ground electronic state of  $\text{OH}(X^2\Pi_{3/2, 1/2})$ .

Quoted values of the rotational temperatures determined from the airglow OH spectrum are in reasonable agreement with the kinetic temperature at the height of the maximum emission determined from rocket measurements (Packer, 1961). The vibrational temperature does not correspond to the ambient kinetic temperature: Krassovsky and Shefov (1965) have determined vibrational temperatures from the OH airglow emissions of approximately  $10,000^\circ\text{K}$ .

In previous studies it has been assumed that the OH emissions originate from molecules in rotational equilibrium with the ambient atmosphere. However, recent observations (Harrison et al., 1970) have shown that the rotational temperature determined from different lines in a given vibration-rotation band is not constant. The purpose of the present work has been to investigate this deviation from isothermal, or equilibrium, behaviour.

### 1.3 Summary of Presentation

In Chapter II, the relevant spectroscopy is presented, and the possible methods of determining spectral temperatures are discussed. A brief survey of the important results of previous OH investigations is included.

In Chapter III, an attempt is made to explain the observed deviation from isothermal behaviour in terms of effects occurring when there is rotational equilibrium in the emitting

molecules. The effect of variation in local kinetic temperature over the OH emission region is considered, and is found to contribute to the deviation from isothermal behaviour. The contribution is not sufficient to explain fully the observations. Other effects that might influence the rotational temperature determination are also considered. It is shown that the observations cannot be explained if the emitting population is in rotational equilibrium.

Non-equilibrium effects are considered in Chapter IV. A rotational relaxation theory is proposed which can be used to calculate the emission spectrum of molecules that are not in rotational equilibrium.

In Chapter V, the rotational relaxation theory is applied to the OH molecules in the upper atmosphere, and calculated rotational temperatures are found to be in agreement with observations. A qualitative discussion of relaxation in the vibrational populations is given. It is found that the relaxation theories can explain qualitatively a number of observed features of the OH nightglow emissions. In Chapter VI, a summary of the work is presented, and possible extensions of the present work are considered.



## CHAPTER II

### SPECTROSCOPY AND ROTATIONAL TEMPERATURES

#### 2.1 Introduction

If a molecular species is in thermal equilibrium with the ambient medium, the population distribution among the rotational energy levels is described by a Boltzmann distribution. The rotational populations, and hence the temperature, may be derived from measured emission intensities of the rotational lines in the molecular spectrum.

The emission intensity of a rotational line depends on both the population of the excited state and the appropriate radiative transition probability, (the Einstein coefficient for spontaneous emission). The populations in the various rotational levels depend on both the energies of these levels and the quantum numbers that describe the levels. Thus, the calculation of the intensity of an emitted line in a molecular spectrum requires a knowledge of the rotational levels available to the molecule.

#### 2.2 Energy Levels

##### 2.2.1 Angular momenta

The total angular momentum of a diatomic molecule,  $\vec{J}$ , is composed of contributions from the electronic orbital angular momentum,  $\vec{L}$ , the electronic spin angular momentum,  $\vec{S}$ , and the nuclear rotational angular momentum,  $\vec{N}$ ; the contribution from nuclear spin may be disregarded (Herzberg, 1950). The manner in which these component angular momenta are coupled

(or interact) determines the value of  $\vec{J}$ , and the possible electronic and rotational energy states available to the molecule.

### 2.2.2 Coupling of angular momenta

The different modes of coupling were first studied by Hund (1927). In Hund's case (a) coupling, the interaction between the nuclear rotational angular momentum  $\vec{N}$  and the electronic angular momenta  $\vec{L}$  and  $\vec{S}$  is weak. The electronic angular momenta are strongly coupled to the internuclear axis of the molecule, and their components along the internuclear axis,  $\vec{\Lambda}$  and  $\vec{\Sigma}$ , become physically useful quantities, with quantum numbers  $\Lambda$  and  $\Sigma$ . The vectors  $\vec{\Lambda}$  and  $\vec{\Sigma}$  are combined to form  $\vec{\Omega}$ , the total electronic angular momentum, with quantum number,

$$\Omega = |\Lambda + \Sigma| \quad (2.1)$$

The total angular momentum of the molecule,  $\vec{J}$ , is then given by the sum of  $\vec{\Omega}$  and the nuclear rotational angular momentum:

$$\vec{J} = \vec{\Omega} + \vec{N} \quad (2.2)$$

As  $\vec{N}$  is, by definition, perpendicular to the internuclear axis,  $\vec{\Omega}$  is the component of  $\vec{J}$  along that axis. It follows that the total angular momentum quantum number ( $J$ ) obeys the relation,

$$J = \Omega, \Omega+1, \Omega+2 \dots \quad (2.3)$$

Due to the possible orientations of the spin angular momentum  $\vec{S}$  relative to the internuclear axis, there are  $2S+1$  possible values of  $\Sigma$ . Thus, there are  $2S+1$  values of  $\Omega$  for each  $\Lambda$ . The degeneracy in the corresponding energy levels is removed by

the coupling between  $\vec{L}$  and  $\vec{S}$ . For molecules with ( $S = 1/2$ ) (e.g.  $\text{OH}(^2\Pi)$ ), the spin multiplicity is:

$$(2S+1) = 2 \quad (2.4)$$

so that for a given value of  $\Lambda$  there are two sets of rotational energy levels, known as spin doublet levels. For a given electronic state ( $\Lambda$  constant) and spin orientation ( $\Sigma$  constant), the quantum number  $J$  specifies the rotational energy levels. The energies of these levels, for a rigid rotator, are (Herzberg, 1950),

$$F_v(J) = B_v[J(J+1) - \Omega^2] \quad (2.5)$$

where  $B_v$  is the rotational constant for the molecule. The two values of  $\Omega$  (if  $S=1/2$ ) specify the spin doublet levels.

In Hund's case (b) coupling, the electron orbital angular momentum  $\vec{L}$  is strongly coupled to the internuclear axis while the electron spin angular momentum  $\vec{S}$  is only weakly coupled. In this case, the vector  $\vec{\Sigma}$  is not defined, and the vectors  $\vec{L}$  and  $\vec{N}$  are combined to give the "total angular momentum without spin",  $\vec{K}$ . As  $\vec{N}$  is perpendicular to the internuclear axis,  $\vec{L}$  is the component of  $\vec{K}$  along the axis, and the quantum numbers obey the relation,

$$K = \Lambda, \Lambda+1, \Lambda+2, \dots \quad (2.6)$$

For a given electronic state ( $\Lambda = \text{constant}$ ), the quantum number  $K$  specifies the rotational energy level.

The total angular momentum of the molecule is,

$$\vec{J} = \vec{K} + \vec{S} \quad (2.7)$$

and the total angular momentum quantum number is given by,

$$J = K+S, K+S-1, \dots, |K-S| \quad (2.8)$$

For each value of  $K$  there are  $2S+1$  values of  $J$ . The degeneracy in the rotational energy levels is removed by the small coupling between  $\vec{S}$  and  $\vec{K}$ , which causes a small splitting of the levels with different  $J$  values for a given  $K$ .

In both case (a) and case (b) coupling, the interaction between  $\vec{N}$  and  $\vec{L}$  is ignored. However, in real molecules there is a small coupling which increases with increasing rotational energy. This causes a splitting into two components for each  $J$  value. The splitting of the energy levels ("Λ doubling") is always small, and for the OH molecule is less than  $1 \text{ cm}^{-1}$ \*

### 2.2.3 Coupling intermediate between case (a) and case (b)

The coupling of the angular momenta in the ground electronic state of the OH molecule is intermediate between case (a) and case (b). For the lower rotational energy levels, the coupling approximates to case (a). As the nuclear rotation increases, the electron spin angular momentum becomes uncoupled from the internuclear axis (and therefore from  $\vec{\Lambda}$ ) and for the higher rotational energy levels case (b) is the more accurate description. Since the multiplet splitting in

---

\*Following spectroscopic practice, the numerical values of energies are expressed in this work in terms of the wave numbers of (hypothetical) photons with the given energy. The energy  $E$ , in erg, may be determined from the equation:

$$E = hc\bar{\nu},$$

where  $h$  is Planck's constant,  $c$  is the speed of light, and  $\bar{\nu}$  is the photon wave number.

the rotational energy levels depends on the coupling between  $\vec{L}$  and  $\vec{S}$ , the splitting decreases in magnitude with increasing rotational energy.

The rotational energy levels for case (a) coupling are specified by quantum number  $J$ , while for case (b) the levels are specified by quantum number  $K$ . This leads to a dual system of quantum number notation for the intermediate coupling case. The lower rotational energy levels may be assigned  $K$  values by extending the quantum number system from the levels where it is applicable. Similarly the upper rotational energy levels may be assigned  $J$  values.

The rotational energy levels for the intermediate coupling case cannot be exactly described by the expressions for either case (a) or case (b). However, Hill and Van Vleck (1928) have developed expressions for the energy levels in intermediate cases. For molecules in the  $^2\Pi$  electronic state, the energy levels may be written (Herman and Hornbeck, 1953),

$$\begin{aligned} F_1(J) &= B_V \left\{ (J+1/2)^2 - 1 - 1/2 [4(J+1/2)^2 + Y_V(Y_V - 4)]^{1/2} \right\} - D_V J^4 \\ F_2(J) &= B_V \left\{ (J+1/2)^2 - 1 + 1/2 [4(J+1/2)^2 + Y_V(Y_V - 4)]^{1/2} \right\} \\ &\quad - D_V (J+1)^4 \end{aligned} \quad (2.9)$$

where the energy subscripts identify the spin doublet component energy levels, and  $B_V$ ,  $D_V$ , and  $Y_V$  are constants for the molecule. In the OH molecule, the  $F_1(J)$  levels correspond to the  $^2\Pi_{3/2}$  states, and the  $F_2(J)$  levels to the  $^2\Pi_{1/2}$  states. As the

rotational energy levels may be described by quantum number  $K$ , equation (2.9) may also be written,

$$\begin{aligned} F_1(K) &= B_v \left\{ (K+1)^2 - 1 - 1/2 [4(K+1)^2 + Y_v(Y_v - 4)]^{1/2} \right\} - D_v (K+1/2)^4 \\ F_2(K) &= B_v \left\{ K^2 - 1 + 1/2 [4K^2 + Y_v(Y_v - 4)]^{1/2} \right\} - D_v (K+1/2)^4. \end{aligned} \quad (2.10)$$

For the  $F_1(K)$  levels,  $J$  and  $K$  are related by

$$K = J - 1/2, \quad (2.11)$$

while for the  $F_2(K)$  levels, the relation is

$$K = J + 1/2. \quad (2.12)$$

Equations 2.9 and 2.10 apply for any degree of coupling between case (a) and case (b), and the  $J$  and  $K$  notations are interchangeable.

#### 2.2.4 Vibrational energy levels

The vibrational motion of a diatomic molecule may be described approximately by a harmonic oscillator. In this model, the two nuclei oscillate along the internuclear axis with a potential energy proportional to the square of the internuclear separation,

$$V(r) = -kr^2 \quad (2.13)$$

where

$$k = 4\pi^2 \mu \nu_{osc}^2, \quad (2.14)$$

$\mu$  is the reduced mass of the system, and  $\nu_{osc}$  is the vibrational frequency. The energy levels of such an oscillator are given

by (Herzberg, 1950),

$$G(v) = \omega(v+1/2) \quad (2.15)$$

where  $\omega = v_{osc}/c$  and  $v$  is the vibrational quantum number.

In a real molecule the potential energy is not a simple quadratic function of the internuclear separation, and the rotational energy levels may be expressed as a power series in  $v$  (Herzberg, 1950),

$$G(v) = \omega_e(v+1/2) - \omega_e x_e(v+1/2)^2 + \omega_e y_e(v+1/2)^3 + \dots \quad (2.16)$$

where  $\omega_e$ ,  $x_e$ ,  $y_e$  are constants for the molecule.

#### 2.2.5 Total energy

The energy levels of a diatomic molecule are determined by the electronic, rotational, and vibrational energies. The electronic motion is in general much more rapid than either the vibrational or rotational motions, so the electronic energy levels may effectively be considered for a stationary molecule. Similarly the vibrational motion is much more rapid than the rotational motion, and may therefore be considered for a non-rotating molecule.

The effect on the energy levels of this behaviour is that for each electronic energy level, there are a number of vibrational energy levels, and with each of these vibrational energy levels there are associated rotational energy levels. The vibration-rotation energy levels (for a given electronic state) for a real diatomic molecule may be written (Herzberg, 1950),

$$E(v,J) = G(v) + F_v(J) \quad (2.17)$$

where  $G(v)$  and  $F_v(J)$  are given by equations 2.16 and 2.9.

## 2.3 Diatomic Spectra

### 2.3.1 Transition selection rules

The spectrum emitted by excited diatomic molecules is determined by the energy levels in the molecule, and the radiative transitions that occur between these levels. The selection rules for radiative transitions are determined from the transition matrix. For electric dipole transitions between electronic-vibration-rotation energy levels the selection rules are given in Table 2.1. The selection rules  $\Delta\Sigma=0$  and  $\Delta S=0$  imply that electric dipole transitions between different spin multiplet levels are forbidden. Transitions for which  $\Delta K \neq \Delta J$  ( $\Delta S \neq 0$ ) are forbidden as electric dipole transitions, but may occur as electric quadrupole transitions.

For a harmonic oscillator, there is the extra selection rule for vibrational transitions,

$$\Delta v = \pm 1 \quad (2.18)$$

For real diatomic molecules this selection rule does not apply, and in general transitions may occur with any value of  $\Delta v$ .

### 2.3.2 Vibration-rotation spectra

Transitions between the vibrational and rotational energy levels in a given electronic state occur in "bands", each of which corresponds to a transition between given vibrational levels. The bands consist of a number of spectral lines, which correspond to transitions between specific rotational



TABLE 2.1  
SELECTION RULES FOR  
ELECTRIC DIPOLE TRANSITIONS

1. Case (a) and Case (b) Coupling:

$$\Delta J = 0, \pm 1 \quad (\text{except } J=0 \nrightarrow J=0)$$

$$\Delta \Lambda = 0, \pm 1$$

$$\Delta S = 0$$

even parity  $\rightarrow$  odd parity

odd parity  $\rightarrow$  even parity

2. Case (a) Coupling Only

$$\Delta \Sigma = 0$$

$$\Delta \Omega = 0, \pm 1$$

3. Case (b) Coupling Only

$$\Delta K = 0, \pm 1 \quad (\Delta K \neq 0, \Lambda = 0 \rightarrow \Lambda = 0)$$

energy levels. The rotational lines in each vibrational band are arranged into separate "branches", corresponding to the different values of  $\Delta J$  (or  $\Delta K$ ). For transitions in  $\Pi$  electronic states ( $\Lambda=1$ ), the J selection rules are  $\Delta J = 0, \pm 1$ , and the branches are labeled P, Q, and R, for  $\Delta J = -1, 0, +1$ .

For molecules which obey Hund's case (a) coupling, the multiplet splitting may be sufficiently large that the multiplet components appear as separate branches. For molecules in which case (b) coupling applies, the multiplet splitting is small, and each line in the branches is split into  $(2S+1)$  spin multiplet components.

### 2.3.3 Vibration-rotation spectrum of OH

The  $\text{OH}(^2\Pi_{1/2,3/2})$  Meinel bands in the airglow arise from transitions between the vibration-rotation energy levels ( $v' \leq 9$ ) in the ground electronic state. The anharmonic nature of the potential function permits transitions between any two vibrational levels, and 45 bands are observed. The two sets of energy levels from the spin splitting correspond to  $\Omega=3/2, 1/2$ . The ground electronic state is inverted, so that the  $\Omega = 3/2$  levels are lower in energy than the corresponding levels for  $\Omega = 1/2$ .

Each OH vibration-rotation band shows the characteristic division into three major branches, P, Q, and R, and due to spin splitting, each of these branches is double. The angular momentum coupling is intermediate between Hund's case (a) and case (b). For low rotational quantum number, the

doublet splitting of the energy levels is large, and results in well separated spin doublet lines. For higher rotational quantum numbers, the doublet splitting of the energy levels decreases, and the wavelength separation between the spin doublet component lines is smaller. Each spin doublet line is further split into two closely spaced components ( $\Lambda$ -doublets) due to the weak coupling between  $\vec{L}$  and  $\vec{N}$ . Twelve satellite branches arise from transitions for which  $\Delta J \neq \Delta K$ , but are very weak in comparison with the twelve principal branches. Neither the  $\Lambda$ -doublets nor the satellite branches have yet been identified in OH airglow spectra.

A theoretical spectrum of the OH(5-2) band calculated for a spectrometer with a slit-width of  $27\text{\AA}$  is shown in Figure 2.1. The P, Q, and R branches are resolved, but the individual rotational lines are only resolved for the P branch, and for these the spin doublet lines are not resolved. The spectrum has been calculated for emissions from molecules in rotational equilibrium at a temperature of  $180^\circ\text{K}$ .

#### 2.3.4 Intensity of emission lines

The intensity of the spectral emission line resulting from a radiative transition between two levels  $n, m$  is given by,

$$I_{nm} = N_n h c \nu_{nm} A_{nm} \quad (2.19)$$

where  $N_n$  is the population of the upper state,  $\nu_{nm}$  is the wave number of the emitted photon,  $h$  is Planck's constant,  $c$  is the speed of light, and  $A_{nm}$  is the Einstein transition

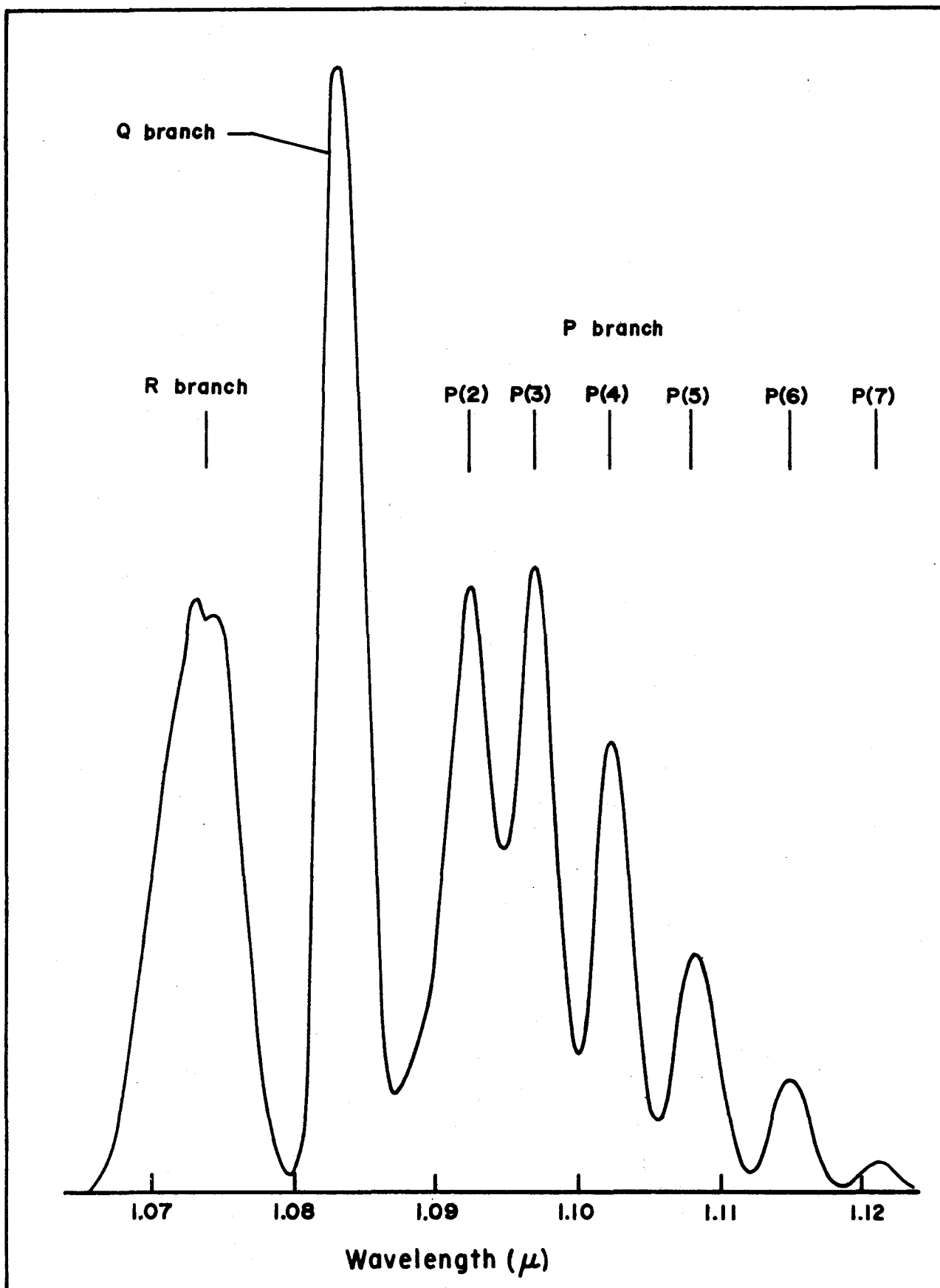


Figure 2.1: OH (5-2) band spectrum calculated for a spectrometer slit width of 27 $\text{\AA}$ , at a temperature  $T = 180^\circ\text{K}$ .

probability for spontaneous emission.

For transitions between non-degenerate levels, the transition probability may be written,

$$A_{nm} = \frac{64\pi^4 \nu_{nm}^3}{3h} |R^{nm}|^2 \quad (2.20)$$

where  $R^{nm}$  is the matrix element of the transition. For transitions between degenerate levels the expression for  $A_{nm}$  (equation 2.20) must be modified. If the emitting molecules are in rotational equilibrium, it can be shown that the emission intensity of a rotational line for a vibrational transition between levels  $v'$ ,  $v''$  is (Herzberg, 1950),

$$I(v', v'', J' J'') = \frac{64\pi^4 c N}{3} \frac{\nu^4(v', v'', J', J'')}{Q_{r'}} \sum |R(v', v'')|^2 \\ \times \exp\left[-\frac{F_{v'}(J') hc}{kT}\right] \quad (2.21)$$

where  $N$  is the total number of molecules in the upper vibrational level,  $Q_{r'}$  is the rotational partition function for the upper state,  $F_{v'}(J')$  is the energy of the upper state,  $T$  is the equilibrium kinetic temperature, and the matrix elements  $R(v', v'')$  are summed over the degenerate rotational levels.

The transition matrix element term depends on the vibrational eigenfunctions of the levels involved in the transition, and on the rotational quantum number  $J$ , due to spatial degeneracy. The  $J$ -dependent part of the transition matrix

term is normally denoted by  $S(J')$ , the "line strength".

If the constant terms in equation 2.21 are combined with the  $J$ -independent part of the transition matrix term and the result expressed as  $C_{em}$ , the emission intensity for a rotational line may be written\*,

$$I(v', v'', J', J'') = C_{em} \frac{v^4(v', v'', J', J'')}{Q_{r'}} S(J') \times \exp\left[-\frac{F_{v', (J')} hc}{kT}\right] \quad (2.22)$$

### 2.3.5 Line strength factors

Simple expressions for the line strengths have been obtained by Hönl and London (1925) for case (a) coupling conditions. For diatomic molecules in an electronic state  $\Lambda > 0$ , the line strengths may be written,

$$\Delta J = +1 \quad S(J') = \frac{(J' + \Omega)(J' - \Omega)}{J'} \quad (\text{R branch})$$

$$\Delta J = 0 \quad S(J') = \frac{(2J' + 1)\Omega^2}{J'(J' + 1)} \quad (\text{Q branch})$$

$$\Delta J = -1 \quad S(J') = \frac{(J' + 1 + \Omega)(J' + 1 - \Omega)}{J' + 1} \quad (\text{P branch}) \quad (2.23)$$

As the OH molecule is not exactly described by case (a) coupling, the values obtained using these formulae are in error.

---

\*In this equation,  $I$  is expressed in energy units. It may be converted to photon units if the term  $v^4$  is replaced by  $(v^3/h)$ .

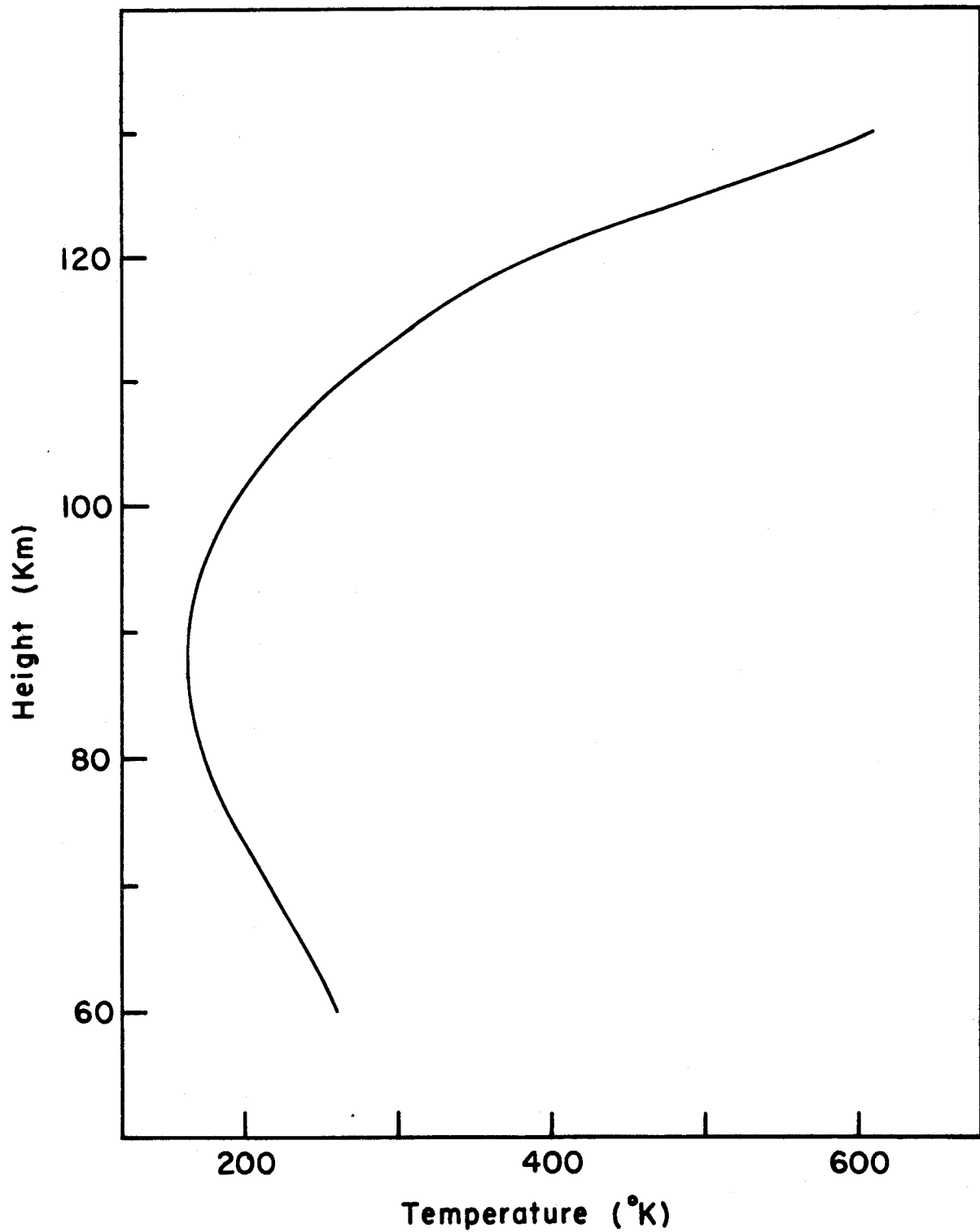


Figure 3.2: Atmospheric temperature profile, summer, 45° latitude (United States Standard Atmosphere tables, 1966).

However, Hill and Van Vleck (1928) have derived analytic expressions for the line strength factors for coupling cases intermediate between cases (a) and (b). Numerical values for the OH molecule have been calculated from the Hill and Van Vleck formulae by Benedict et al. (1953). These values are given in Table 2.2 together with values calculated from Hönl-London formulae (equation 2.23). The agreement between the two sets of values is good for the lower rotational levels, where case (a) coupling is applicable to the OH molecule.

The line strengths given in Table 2.2 have been calculated for transition matrix elements in which interaction between rotational and vibrational energies has been neglected. If the matrix elements are calculated using wave functions which include the interaction between rotational and vibrational motions, a further J dependence is obtained. Herman and Wallis (1955) have shown that the transition matrix elements may be written,

$$|R(v', v'', J', J'')|^2 = |R(v', v'')|^2 F(v', v'', J', J'') \quad (2.24)$$

where  $R(v', v'')$  is the matrix element for a non-rotating oscillator,  $R(v', v'', J', J'')$  is the matrix element for the real molecule, and  $F(v', v'', J', J'')$  is the interaction line strength factor. Hence, the emission intensity of a line from a transition between levels  $(v', J')$  and  $(v'', J'')$  is (in energy units),

$$I(v', v'', J', J'') = C_{em} \frac{\nu^4(v', v'', J', J'')}{Q_{r'}} S(J') F(v', v'', J', J'') \times \exp\left(\frac{-F_{v'}(J')hc}{kT}\right) \quad (2.25)$$



TABLE 2.2  
LINE STRENGTH VALUES

---

(a) OH Molecule, Hill and Van Vleck Formulae

K	$\Omega = 3/2$			$\Omega = 1/2$		
	$S_P$	$S_Q$	$S_R$	$S_P$	$S_Q$	$S_R$
1	0.00	2.30	1.62	0.00	0.67	1.29
2	1.62	1.40	2.90	1.29	0.30	2.34
3	2.90	0.98	4.04	2.34	0.22	3.37
4	4.04	0.73	5.14	3.37	0.19	4.37
5	5.14	0.57	6.21	4.37	0.17	5.38
6	6.21	0.46	7.26	5.38	0.16	6.39
7	7.26	0.37	8.30	6.39	0.15	7.39
8	8.30	0.33	9.32	7.39	0.15	8.40
9	9.32	0.29	10.34	8.40	0.14	9.41
10	10.34	0.26	11.36	9.41	0.14	10.42

(b) Hönl-London Formulae

1	0.00	2.40	1.60	0.00	0.67	1.33
2	1.60	1.54	2.86	1.33	0.27	2.40
3	2.86	1.14	4.00	2.40	0.17	3.43
4	4.00	0.91	5.09	3.43	0.13	4.44
5	5.09	0.75	6.15	4.44	0.10	5.45
6	6.15	0.65	7.20	5.45	0.08	6.46
7	7.20	0.56	8.24	6.46	0.07	7.47
8	8.24	0.50	9.26	7.46	0.06	8.47
9	9.26	0.45	10.29	8.47	0.06	9.47
10	10.29	0.41	11.30	9.47	0.05	10.48

---

In previous analyses of the airglow OH spectra, the F factors have been neglected, as the values were not known. An estimate of the values of the interaction factors is given in Chapter III.

### 2.3.6 Transition probabilities

The total intensities of the different vibrational bands depend on the absolute values of the transition probabilities,  $A_{v',v''}$ , which are unknown for the OH Meinel bands. Relative values of the transition probabilities have been determined from observations of the relative band intensities in OH emission spectra. The most recent values for the relative probabilities have been calculated by Stair et al. (1971) and are listed in Table 2.3. Absolute values have been estimated by comparison with the known values for the HCl molecule (Heaps and Herzberg, 1951). It has been assumed in the present work that the absolute value of the probability for a transition between the vibrational levels 1 and 0,  $A_{10}$ , is  $50 \text{ sec}^{-1}$ .

## 2.4 The Determination of Temperature from Rotational Spectra

### 2.4.1 Graphical method

It has been shown that for thermal equilibrium the intensity of a rotational line (equation 2.22) depends on the equilibrium temperature of the molecular rotational population. Equation 2.22 may be rearranged to give the "rotational temperature" in terms of the intensities of the rotation lines in a given band ( $v',v''$ ),

TABLE 2.3  
RELATIVE TRANSITION PROBABILITIES FOR OH,  $A_{v'v''}$

		v''							
	0	1	2	3	4	5	6	7	8
1	.100E+1								
2	.503E+0	.136E+1							
3	.443E-1	.158E+1	.126E+1						
4	.543E-2	.167E+0	.294E+1	.878E+0					
v' 5	.102E-2	.247E-1	.396E+0	.455E+1	.390E+0				
6	.251E-3	.536E-2	.676E-1	.747E+0	.626E+1	.474E-1			
7	.713E-4	.148E-2	.167E-1	.154E+0	.125E+1	.794E+1	.753E-1		
8	.225E-4	.481E-3	.506E-2	.384E-1	.272E+0	.189E+1	.938E+1	.700E+0	
9	.767E-5	.171E-3	.181E-2	.128E-1	.766E-1	.563E+0	.256E+1	.105E+2	.212E+1

$$\log_e \left[ \frac{I(J')}{S(J')v(J')} \right] = \text{constant} - \frac{F(J')hc}{kT} \quad (2.26)$$

where the "constant" term includes the J-independent terms of equation 2.22, and is constant for a given vibrational band. If the intensities of a number of rotational lines in a given band are measured, and the derived values of the logarithmic term are plotted against the rotational energy levels, the rotational temperature T is obtained from the slope of the graph. For the OH Meinel bands the P branch lines are generally used for the determination of rotational temperatures by the graphical method.

#### 2.4.2 Relative branch intensity method

Due to the difference in the values of the line strengths for the P, Q, and R branches, the relative intensities of these branches vary with temperature. Hence, the rotational temperature may be determined from comparison of observed branch intensity ratios with values calculated for known temperatures.

#### 2.4.3 Spin doublet temperature

For the OH molecule the  $\Pi_{1/2}$  levels have a higher energy than the corresponding  $\Pi_{3/2}$  levels. If the populations of the two sets of rotational levels are in thermal equilibrium the difference in intensity between two corresponding spin doublet lines will be related to the temperature (Meinel, 1950),

$$\frac{I(1/2)}{I(3/2)} = \exp\left(-\frac{Ahc}{kT}\right) \quad (2.27)$$

where  $A = 138 \text{ cm}^{-1}$  for the OH molecule.

The validity of this method depends on the excitation mechanism. As only transitions for which  $\Delta S = 0$  are allowed, it is not possible to redistribute populations between the doublet levels. Thus, if the excitation mechanism does not initially distribute the populations according to the above relation, the derived "temperature" is not a measure of the ambient kinetic temperature.

#### 2.4.4 Comparison of Spectra

If it is assumed that an observed spectrum originates from a rotational population in thermal equilibrium, the kinetic temperature may be determined by comparison with theoretical spectra calculated at known temperatures. This method is a simple extension of the graphical method to more than one branch in the band.

#### 2.5 Survey of Previous Work

Since the identification of the OH bands in the night-glow by Meinel (1950) extensive investigations of rotational temperatures have been undertaken. A complete survey of this work is beyond the scope of this discussion, but some of the results and conclusions are relevant to the present work.

In general, the rotational temperatures derived from the graphical method have suggested that the emitting rotational

populations are in thermal equilibrium. The standard method for determining the rotational temperature has been to obtain the straight line of best fit to the graphical data. In this method any deviation from isothermal behaviour is ignored.

It has been recognized that the temperature determined from OH rotational spectra will be a mean of the atmospheric temperatures over the emission region (McPherson and Vallance Jones, 1960; Krassovsky, 1963). However, it has been claimed that the deviation from isothermal behaviour in rotational temperatures due to the averaging process is small and may be neglected for rotational lines with  $K < 6$  (Shefov, 1961). From considerations of the collision frequency at the height of origin of the OH emissions, it has been concluded that the emitting populations are in thermal equilibrium, (McPherson and Vallance Jones, 1960; Krassovsky, 1963). Hence, it has been assumed that the OH rotational temperatures are a measure of the kinetic temperature in the emitting region. On this assumption it has not been possible to explain the behaviour of the rotational temperatures for the higher vibrational levels, reported by Russian workers, (Krassovsky, 1963). The observed rotational temperatures are  $\sim 350^\circ$  for bands with  $v' = 9$ , which is significantly higher than the average kinetic temperatures in the OH emission region. It was concluded that these rotational temperatures were not a measure of the equilibrium kinetic temperature, due to some chemical deactivation process (Krassovsky and Shefov, 1965).

Recently, observations have been published which

indicate a departure from isothermal behaviour of rotational temperatures for lines with  $K < 6$  (Harrison et al., 1970).

CHAPTER III  
NON-ISOTHERMAL BEHAVIOUR IN  
OH AIRGLOW ROTATIONAL TEMPERATURES  
1. EQUILIBRIUM CONDITIONS

### 3.1 Introduction

In the early investigations of the OH airglow, estimates of the height of the emissions were made using the Van Rhijn method. For accurate results this technique requires that the emissions be confined to a narrow layer, and that they be spatially homogeneous. The failure to recognize that the OH emissions did not satisfy these requirements accounts for the considerable spread in the published values of the emission height (Chamberlain, 1961). Subsequent rocket measurements have shown that the OH nightglow is emitted from a region centered near 90 km with a half width of approximately 20 km (Harrison, 1970). As a number of authors have already noted (McPherson and Vallance Jones, 1960; Shefov, 1961; Krassovsky, 1963; Harrison et al., 1970), the rotational temperature calculated from the airglow spectra will be a weighted average of the atmospheric temperatures in the emission region if the OH rotational populations are in thermal equilibrium with the surrounding atmosphere.

### 3.2 Profile Weighted Spectral Temperatures

#### 3.2.1 Observed OH emission height profiles

The first OH emission profile measurement was made by Heppner and Meredith (1958) with a rocket-borne photometer designed to measure the OI 6300<sup>0</sup>Å emission, which also admitted part of the OH(9-3) band in the same spectral region.



TABLE 3.1  
OH NIGHTGLOW EMISSION PROFILE MEASUREMENTS

---

Date	Altitude	Wavelength	Reference
November, 1958	75 km	1.6 $\mu$	Lowe, 1960
November, 1959	83 km	7220 - 7370 $\text{\AA}$	Packer, 1961
November, 1959	89 km	7400 - 10200 $\text{\AA}$	Packer, 1961
September, 1960	78, 85 km	9100 - 10700 $\text{\AA}$	Tarasova, 1961
April, 1966	97 km	7210 - 7450 $\text{\AA}$	Baker and Waddoups, 1967
October, 1969	95 km	8305 - 8455 $\text{\AA}$	Harrison, 1970

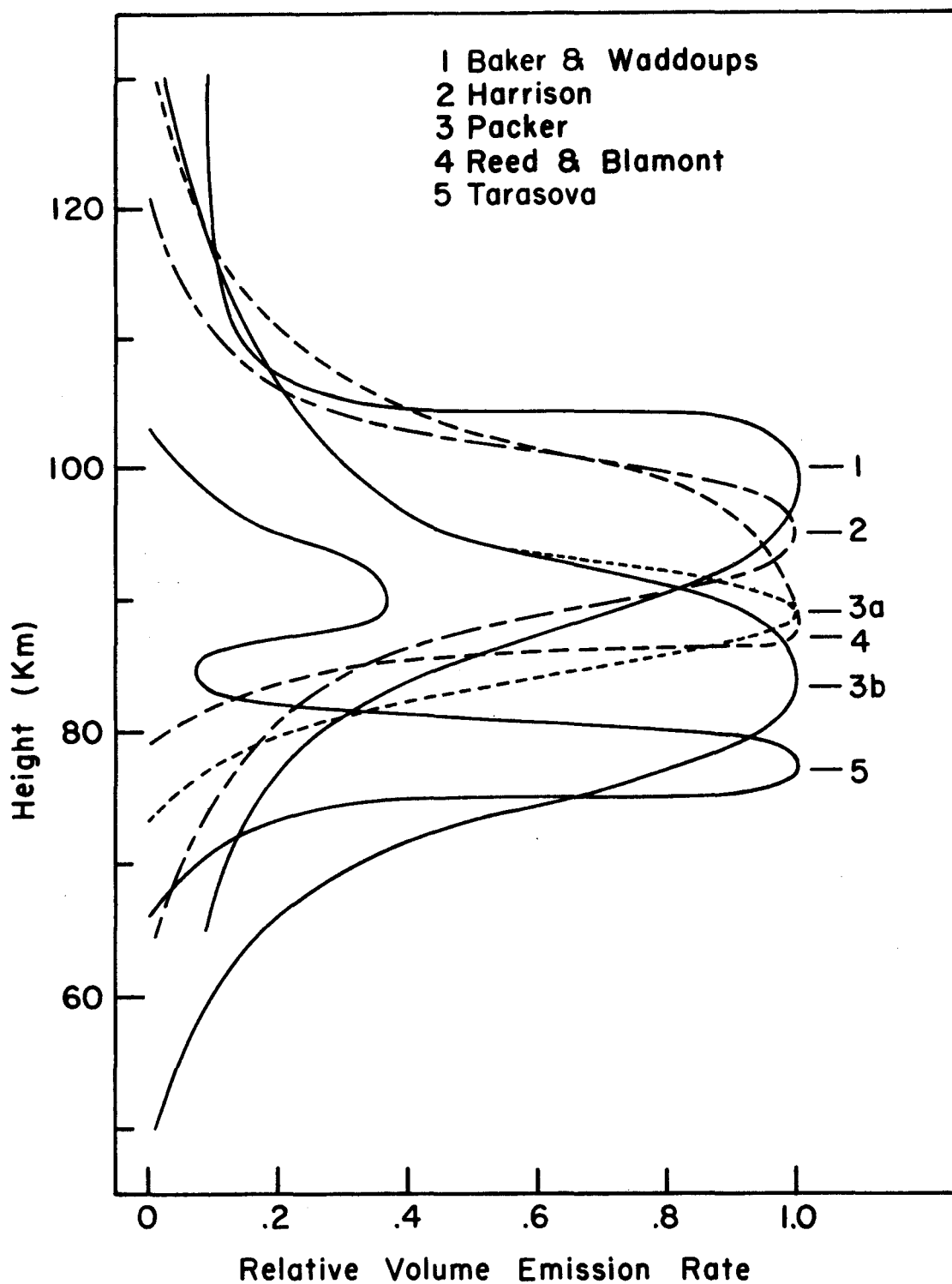


Figure 3.1: Measured OH emission height profiles.  
(Subsequent references to the Packer profile relate to curve 3b.)

Subsequent rocket measurements of the OH emission profile in the nightglow have been made by Lowe (1960), Packer (1961), Tarasova (1961), Baker and Waddoups (1967) and Harrison (1970), and in the twilight by Llewellyn and Evans (1971). The data from the satellite OGO-II have provided further OH profiles (Reed and Blamont, 1967) from the 6300Å photometer. The results of the nightglow measurements are shown in Figure 3.1 and Table 3.1, and indicate that in general the OH emission originates from altitudes between 60 km and 130 km, with a single intensity maximum near 90 km.

### 3.2.2 Calculated rotational spectra

The atmospheric temperature profile (Figure 3.2) exhibits a minimum near 85 km, which is approximately at the same height as the maximum of the OH emission. If the rotational temperature is a profile averaged temperature, weighted in favour of the temperature at the height of maximum emission, then the temperature determined from the OH spectra should be approximately the minimum atmospheric temperature.

To investigate the effect of this averaging process on measured rotational temperatures an integrated OH spectrum has been computed. If the emitting molecules are in thermal equilibrium, the intensity (photon units) of a rotational line in the OH spectrum emitted from a height  $z$  may be written (c.f. equation 2.22),

$$I(K,z) = P(z) \frac{C_{em}}{Q_{r,1}(z)} \nu^3(K) S(K) \exp\left[\frac{-F(K)}{KT(z)}\right] \quad (3.1)$$

where  $P(z)$  is the volume emission rate at height  $z$ , and  $T(z)$  is the ambient temperature at height  $z$ . The rotational partition function  $Q_r$  is a function of temperature and, therefore, also of height. The "integrated" intensity of this spectral line, or the intensity contribution from emissions at all heights, is given by,

$$I(K) = \int_{Z_1}^{Z_2} I(K, z) dz \quad (3.2)$$

The limits of the integral are defined by the upper and lower limits of the OH emission profile, and equation 3.2 may be rewritten as,

$$I(K) = \int_{Z_1}^{Z_2} \frac{P(z) C_{em} v^3(K) S(K)}{Q_r} \exp\left[\frac{-F(K)}{kT(z)}\right] dz \quad (3.3)$$

As  $P(z)$  and  $T(z)$  do not have simple analytic forms, this integral may be evaluated by approximating to a summation,

$$I(K) = \sum_{i=1}^N P_i v^3(K) S(K) \exp\left[\frac{-F(K)}{kT_i}\right] \Delta z \quad (3.4)$$

This corresponds to dividing the emission profile into  $N$  thin layers (thickness  $\Delta z$ ), each of which is considered as emitting with intensity  $P_i$  at a temperature  $T_i$ . The summation may be performed for each rotational line in the band and the resulting spectrum analysed in the usual way to determine rotational temperatures.

The rotational temperature graph for the P1 branch of such a spectrum is shown in Figure 3.3. In this calculation,

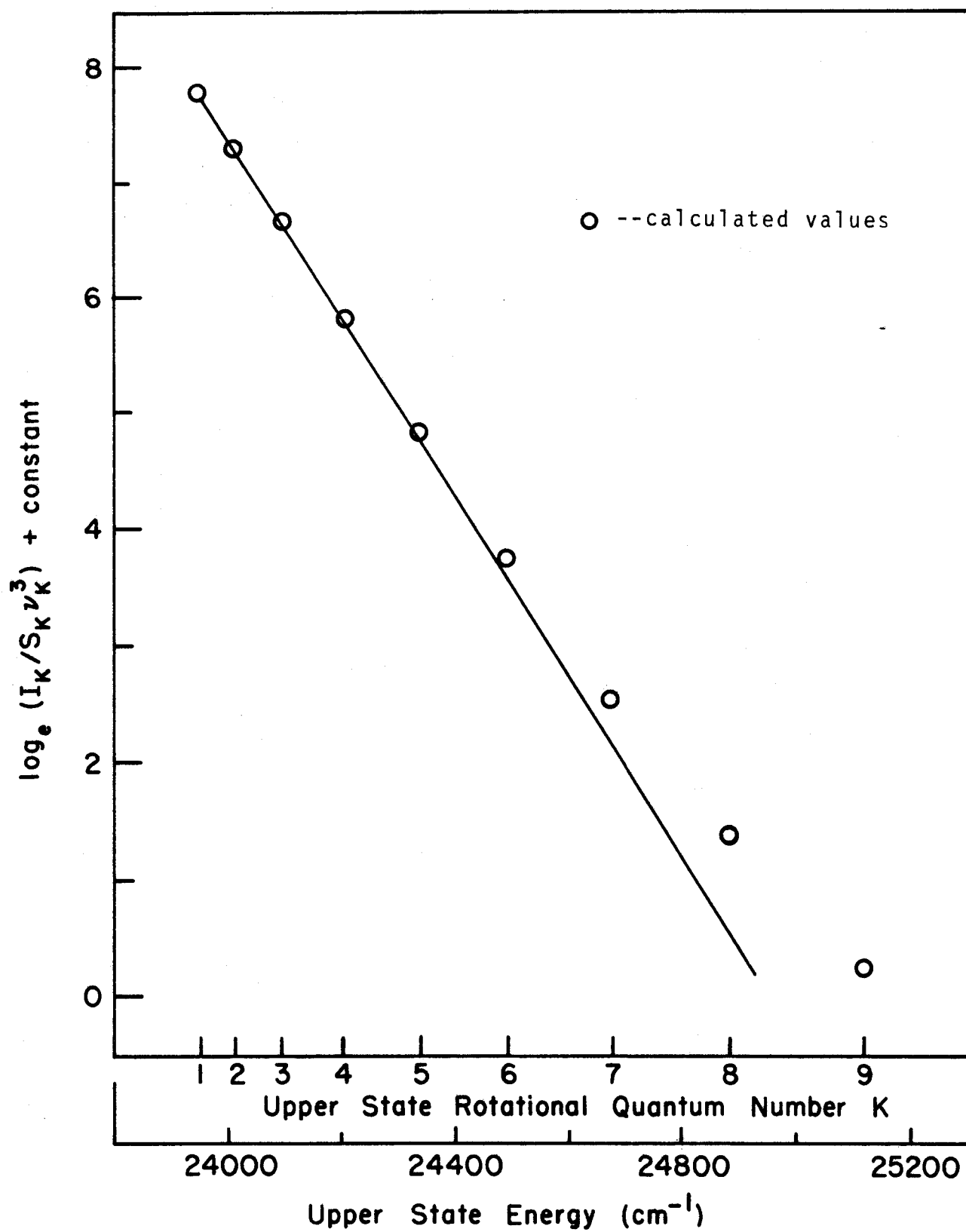


Figure 3.3: Rotational temperature graph for the P1 lines, (8-4) band, calculated for the Packer (1961) emission height profile.

the emission height profile measured by Packer (1961) and the United States Standard Atmosphere (1966) temperature profile (45° latitude, summer) were used. It is evident from Figure 3.3 that OH spectra calculated using the weighted averaging process do not give a constant rotational temperature. The deviation from isothermal behaviour is in the same sense as that for the spectra obtained by Harrison *et al.* (1970), with higher temperatures for lines originating from higher values of  $K''$ . The derived temperature values for the different P lines are given in Table 3.2 together with the values obtained from ground-based nightglow observations. Each temperature is calculated from the intensity ratio of two lines in the P branch with the subscripts identifying the appropriate lines (Harrison *et al.*, 1970) (c.f. equation 3.13, page 44). For lower values of the rotational quantum number  $K''$  (the brighter lines in the P branch), the rotational temperature for the synthetic spectrum is 185°K. It should be noted that although the atmospheric temperature varies between 160°K and 600°K over the height range of the OH emission, the rotational temperature for these lines is approximately that for the atmospheric temperature at the emission peak. This is in agreement with that expected from qualitative considerations. However, the deviation from isothermal behaviour in the rotational temperatures is considerably larger for the observed spectra than for the calculated spectrum.

Synthetic spectra were computed for other measured emission height profiles, and in all cases the non-isothermal

TABLE 3.2  
COMPARISON OF THEORETICAL AND OBSERVATIONAL  
ROTATIONAL TEMPERATURES

		Rotational Temperature (°K)							
		T <sub>23</sub>	T <sub>24</sub>	T <sub>25</sub>	T <sub>26</sub>	T <sub>27</sub>	T <sub>28</sub>	T <sub>29</sub>	T <sub>210</sub>
Theoretical Spectrum (8-4) Band		183.4	184.7	186.7	189.6	193.9	200.3	209.6	222.5
Experimental Observations (4-1) Band (Harrison et al., 1970)		193±3	201±2	232±	263±4	---	---	---	---
		179±3	184±2	217±	246±3	---	---	---	---
		170±3	175±2	202±2	233±3	---	---	---	---

behaviour was evident. For an emission profile with an intensity peak at a higher altitude than the atmospheric temperature minimum, a higher value for the rotational temperature is obtained from lines with a low rotational quantum number.

It is evident from Figure 3.1 that the "Packer" profile has the greatest vertical extent of the observed nightglow emission profiles. Therefore, calculations of the averaged spectrum for this profile indicate the maximum contribution from the weighted averaging process to the deviation from isothermal behaviour. For emission profiles of smaller vertical extent a smaller variation occurred in the rotational temperatures for the P branch lines. This is expected as the range in atmospheric temperature is smaller for such profiles.

### 3.3 Atmospheric Profiles from Ground Based Measurements

The mathematical form of equations 3.3 and 3.4 suggests that if two of the three quantities  $I(K)$ ,  $P(z)$  and  $T(z)$  are known, then the third may be calculated. For the case where  $I(K)$  is the unknown, the calculation has been described in section 3.2.2. If the partition function  $Q_r$  is expanded as a function of  $K$  then equation 3.3 may be written as,

$$I(K) = \int_{z_1}^{z_2} \frac{P(z) C_{em} v^3(K) S(K) \exp[-F(K)/kT(z)]}{\sum_K (2K+1) \exp[-F(K)/kT(z)]} dz \quad (3.5)$$

This equation is an integral equation of the first kind. The intensities  $I(K)$  can be measured for a number of different lines in a given band, and if  $P(z)$  is known, or assumed, it



should be possible to solve equation 3.5 for  $T(z)$ , the atmospheric temperature profile. In practice, the solution is very unstable and the probability of obtaining an accurate profile is small. This instability is suggested by the fact that the use of several different emission height profiles,  $P(z)$ , gave rise to only small changes in the measured values of the rotational line intensities,  $I(K)$ . Numerical methods have been developed for solving equations such as 3.5, but their accuracy is low (Twomey, 1965; Kozlov, 1966), which suggests that there is little advantage to be gained from attempting to derive atmospheric profiles in this manner.

### 3.4 Vibration Rotation Interaction and Line Strengths

#### 3.4.1 Introduction

In the analysis of both observational and theoretical spectra, the rotation dependent parts of the vibration transition matrix (the so-called F factors)\* have been neglected. It is possible that the neglect of these factors may introduce a spurious deviation from isothermal behaviour in the measured rotational temperatures. This effect would not necessarily appear in the analysis of the computed spectra, as the  $S_F(K)$  factors were neglected in the intensity calculations. The reason for neglecting the vibration rotation interaction line strength factors is that their values are not accurately known for the OH molecule. To permit an accurate analysis of the observed spectra it is necessary to estimate the effect that the  $S_F(K)$  factors might have on the rotational temperature

---

\*Due to the use of the notation  $F(K)$  for the rotational term energy, the vibration rotation interaction line strengths will be written here as  $S_F(K)$ .

determination.

### 3.4.2 Analysis for estimated interaction factors

Wallace (1962) has noted that rotational temperatures reported by Shefov (1961) and analysed neglecting the  $S_F(K)$  factors were isothermal. This has been interpreted to indicate that for the (4-1) and (5-2) bands the  $S_F(K)$  factors are close to unity. In view of the recent results of Harrison et al. (1970) for the (4-1) band, which indicate a non-isothermal behaviour, this assumption must be reconsidered.

Herman and Wallis (1955) have shown that to a first approximation for the fundamental bands,

$$S_F(K) = 1 + 4\gamma\theta m \quad (3.6)$$

where  $m = K$  for the P lines,

$$= -(K+1) \text{ for the R lines,}$$

$$\gamma = \frac{2B_e}{\omega_e},$$

and

$$\theta = \frac{M_0}{M_1 r_e}.$$

$M_0$ ,  $M_1$  are the first two terms in the Taylor expansion of the dipole moment,  $M(r)$ , and  $r_e$  is the equilibrium internuclear separation. For the overtone bands ( $\Delta v = n$ ),  $\gamma$  may be expressed as (Cashion, 1963),

$$\gamma = \frac{2B_e}{n\omega_e} \quad (3.7)$$

and equation 3.6 may be written,

$$S_F(K) = 1 + \frac{8B_e m\Theta}{n\omega_e} . \quad (3.8)$$

For the values of  $B_e$  and  $\omega_e$  for the OH molecule (Herzberg, 1950), the interaction factor for the P branch lines in the (4-1) band is,

$$S_F(K) = 1 + 0.013\Theta K \quad (3.9)$$

The value of  $\Theta$  depends on the dipole moment which has been measured for the OH molecule by Phelps and Dalby (1965). They obtained values for the first three coefficients in the expansion of  $M(r)$ , from which  $\Theta$  may be calculated. On the basis of these measurements the value of  $\Theta$  is  $-1.0 \pm .5$ . The large experimental uncertainties limit the usefulness of this value in the calculation of the vibration-rotation interaction line strength factors. However, an estimate may be made of the magnitude of the factors. If  $\Theta_{OH} = -1.0$ , then for the (4-1) band,

$$S_F(K) = 1 - 0.013K \quad (3.10)$$

and for the P(6) lines in that band,  $S_F(6) = 0.92$ . This indicates that the neglect of the interaction line strength factors in the analysis of (4-1) band observational spectra will cause an  $8(\pm 4)\%$  error in the effective line strength values, for the highest values of  $K$  observed in airglow spectra.

To estimate the effect on the rotational temperatures of errors in the effective line strength values, spectra were computed for total line strengths given by the expression,

$$S'(K) = S(K)(1 + \epsilon K) \quad (3.11)$$

for different values of  $\epsilon$ , and at a constant temperature  $T = 200^\circ\text{K}$ . These spectra were then analysed using the simple line strengths,  $S(K)$ , to determine rotational temperature; the results are given in Table 3.3. The value  $\epsilon = -0.01$  corresponds to the estimated values of  $S_F(K)$  for the (4-1) band.

It is apparent from Table 3.3 and equation 3.10 that the effect on the rotational temperature is small for the higher overtone bands, (small  $\epsilon$ ). This indicates that neglecting the  $S_F$  factors does not contribute to the disparity between the observed deviation from isothermal behaviour, and that calculated from the atmospheric temperature averaging process. If the assumed value of  $\theta$  is correct, the  $S_F$  factors are only important in the fundamental and first overtone band spectra. A complete discussion is not possible until a more precise measurement is made of the dipole moment for the OH molecule.

### 3.4.3 Other uncertainties in the line strengths

As the  $\text{OH}(^2\Pi)$  level is intermediate in coupling between Hund's case (a) and case (b), the line strengths are not given exactly by the Hönl-London formulae. However, Hill and Van Vleck (1928) have developed formulae for intermediate coupling cases. Benedict et al. (1953) have calculated the line strengths for the  $\text{OH}(^2\Pi-^2\Pi)$  transitions from the Hill and Van Vleck formulae, and it is these values which have been used in all calculations in the present work. It may, therefore, be assumed that errors in the adopted line strength values are small. The effects of such errors have been considered

TABLE 3.3  
THE EFFECT OF ERRORS IN LINE STRENGTH VALUES  
(Equilibrium Temperature 200°K)

Rotational Temperature (°K)									
$\epsilon$	$T_{23}$	$T_{24}$	$T_{25}$	$T_{26}$	$T_{27}$	$T_{28}$	$T_{29}$	$T_{210}$	
.005	202.2	201.8	201.6	201.4	201.2	201.1	200.9	200.9	
.01	204.4	203.7	203.1	202.7	202.4	202.1	201.9	201.7	
.02	209.0	207.3	206.2	205.3	204.7	204.1	203.7	203.4	
.05	222.9	218.2	215.0	212.7	210.9	209.6	208.5	207.6	
-.005	197.8	198.2	198.4	198.6	198.8	198.9	199.0	199.1	
-.01	195.6	196.3	196.8	197.2	197.5	197.7	197.9	198.1	
-.02	191.3	192.6	193.6	194.3	194.9	195.4	195.7	196.0	
-.05	178.7	181.5	183.5	185.0	186.2	187.1	187.1	188.3	

effectively in the discussion of the  $S_F(K)$  factors, where it was shown that uncertainties of 10% in  $S(K)$  have only a small effect on the derived rotational temperature.

### 3.5 The Effect of Failure to Resolve the Spin Doublet Components

The rotational temperatures reported by Harrison et al. (1970) were obtained from spectra measured with a spectral half width of  $27\text{\AA}$ . In these spectra the P branch spin doublets were not resolved. If the rotational temperatures are derived using the line strengths for the P1 lines, which differ from those for the P2 lines, it is probable that significant errors will be introduced into the temperature values obtained. To estimate the magnitude of the errors in the derived rotational temperatures, a theoretical spectrum was calculated for emission at a single temperature and convolved to synthesize the output of a spectrometer with a  $27\text{\AA}$  spectral half width. The computer spectrum was then analysed in the manner described above. The results of these calculations for an equilibrium temperature of  $200^\circ\text{K}$  are given in Table 3.4. It is apparent that the deviation from isothermal behaviour is in the opposite sense to the observed in the nightglow, and that analysis in this manner of unresolved spectra would not contribute to the observed nightglow effect. It should be noted that rotational temperatures obtained in this way cannot be compared directly with those obtained from spectra where the spin doublets are resolved.

TABLE 3.4  
THE EFFECT OF USING P1 LINE STRENGTHS IN THE ANALYSIS OF  
UNRESOLVED P LINE SPIN DOUBLETS  
(Equilibrium Temperature 200°K; Spectrometer Slit Width 27Å)

Rotational Temperature (°K)						
T <sub>23</sub>	T <sub>24</sub>	T <sub>25</sub>	T <sub>26</sub>	T <sub>27</sub>	T <sub>28</sub>	T <sub>29</sub>
219.5	218.1	215.0	212.8	210.8	209.2	207.9
						206.8

To avoid the difficulty caused by the above method of analysis, the rotational temperatures presented by Harrison et al. (1970) were determined by comparison of the observed line intensity ratios with those from synthetic spectra calculated for a  $27\text{\AA}$  spectral slit width. This procedure takes into account the line strengths of both spin doublets, and the temperatures may, therefore, be compared with those derived from resolved P lines.

### 3.6 The Effect of Background on Rotational Temperature Determination

In the measurement of the intensities of spectral lines the lowest intensity lines observed are determined by the instrumental sensitivity and background noise. The low intensity lines are subject to the greatest uncertainty in measurement. As it is these lines which have been found to deviate most from isothermal behaviour, it is important to determine the effect of measurement uncertainties on the results.

From equation 2.22 the ratio of the intensities  $R$  (in photon units) of two emission lines may be written as,

$$R = \frac{I(K_1)}{I(K_2)} = \frac{S(K_1)\nu^3(K_1)}{S(K_2)\nu^3(K_2)} \exp\left[-\frac{F(K_2)-F(K_1)}{kT}\right] \quad (3.12)$$

This equation may be transposed to give,

$$T = \frac{[F(K_2)-F(K_1)]}{k \log_e \left[ R \frac{S(K_2)\nu(K_2)^3}{S(K_1)\nu(K_1)^3} \right]} \quad (3.13)$$



from which it can be shown that,

$$\frac{\Delta T}{T} = \frac{\Delta R}{R} \left[ \frac{kT}{F(K_1) - F(K_2)} \right] \quad (3.14)$$

P1 branch rotational temperatures have been computed from spectra obtained by adding constant amounts of "noise" to a spectrum calculated for a temperature of 200°K.\* The results are given in Table 3.5, with the noise value expressed in terms of the intensity of P1(10) line. The temperatures listed in parentheses correspond to lines that would be masked by the noise. The calculations indicate that insufficient correction for background in the observed spectra can cause a deviation from isothermal behaviour similar to that observed by Harrison et al. (1970), although smaller in magnitude. Similar arguments show that overcorrection for background continuum in observed spectra will lead to an underestimate of the deviation from isothermal behaviour.

It should be noted that the results of Harrison et al. (1970) have been carefully corrected for background continuum, and the maximum uncertainty in the rotational temperatures is  $\sim \pm 5^\circ\text{K}$ . Therefore, the observed deviation from isothermal behaviour is real.

### 3.7 Self-absorption

Self-absorption of the emitted radiation by ground state molecules is of considerable importance in the rotational spectrum of  $\text{OH}(^2\Sigma^+ - ^2\Pi)$  emissions in laboratory flames, where

---

\*This analysis is equivalent to determining rotational temperatures from spectra in which the background continuum is not negligible.

TABLE 3.5  
THE EFFECT OF BACKGROUND ON ROTATIONAL TEMPERATURES  
(Equilibrium Temperature 200°K)

Background (fraction of P1(10) line intensity)	Rotational Temperatures (°K)						
	T <sub>23</sub>	T <sub>24</sub>	T <sub>25</sub>	T <sub>26</sub>	T <sub>27</sub>	T <sub>28</sub>	T <sub>29</sub> T <sub>210</sub>
0	200	200	200	200	200	200	200 200
.5	199.8	200.0	200.1	200.1	200.3	200.8	202.6 209.7
1.0	199.7	200.1	200.1	200.3	200.6	201.5	205.0 (217.1)
5.0	199.6	200.2	200.5	201.2	202.7	207.3	(220.7) (251.0)
20.0	199.0	200.7	202.1	204.6	210.4	(225.0)	(256.3) (304.9)
100.0	196.1	203.2	209.9	220.9	(242.6)	(282.2)	(340.6) (412.6)

it has been claimed to cause the considerable deviation from isothermal behaviour that is observed (Broida, 1955). It is also important in the infra-red atmospheric bands of  $O_2(^1\Delta_g - ^3\Sigma_g^-)$  at  $1.27\mu$ . The large number of ground state oxygen molecules in the lower atmosphere allow only 6% of these emissions to be transmitted to sea level, and with a considerably modified spectrum (Evans et al. 1970). It is, therefore, of interest to determine the effect of self absorption in the OH airglow spectrum.

The energy absorbed per unit cross section area for a transition from a level  $m$  to a level  $n$  is given by (Herzberg, 1950),

$$I_{abs}^{nm} = I_0^{nm} N_m B_{mn} h\nu_{nm} \Delta x \quad (3.15)$$

where  $I_0^{nm}$  is the incident radiation intensity (energy units) per unit area,  $N_m$  is the number of absorbing molecules per unit volume,  $B_{mn}$  is the Einstein transition probability for absorption,  $h$  is Planck's constant,  $\nu_{nm}$  is the wave number of the radiation, and  $\Delta x$  is the thickness of the absorbing medium. The coefficient  $B_{mn}$  is related to the spontaneous emission transition probability  $A_{nm}$  by,

$$B_{mn} = \frac{A_{nm}}{(8\pi h c \nu_{nm}^3)} \quad (3.16)$$

For the OH Meinel bands,  $\nu_{nm} \sim 10^4 \text{ cm}^{-1}$  and  $A_{nm} \sim 50 \text{ sec}^{-1}$ , so that  $B_{mn} \sim 10^4 \text{ cm}^2 \text{ erg}^{-1} \text{ sec}^{-1}$ ; for the ultra-violet OH( $^2\Sigma^+$ ) bands,  $A_{nm} \sim 10^6 \text{ sec}^{-1}$ , and  $\nu_{nm} \sim 3 \times 10^4 \text{ cm}^{-1}$ , and hence  $B_{mn} \sim 7 \times 10^6 \text{ cm}^2 \text{ erg}^{-1} \text{ sec}^{-1}$ . It is apparent that the absorption probability is much

lower for the infra-red airglow OH bands than for the ultra-violet OH flame spectra.

If equation 3.15 is written to give the fraction of radiation absorbed,

$$\frac{I_{\text{abs}}^{\text{nm}}}{I_0^{\text{nm}}} = N_m B_{mn} h \nu_{nm} \Delta x, \quad (3.17)$$

the effect of self-absorption on the OH airglow spectrum may be calculated. Nicolet (1970) has shown that the number density of OH molecules in the atmosphere is  $\sim 10^7 \text{cm}^{-3}$ , and if these are assumed to be confined to a homogeneous layer of 20 km thickness the fraction of the radiation absorbed is  $\sim 10^{-5}$ . Therefore, the effects of self-absorption on the OH airglow emission may be neglected.

### 3.8 Instrument Effects

#### 3.8.1 Step-scanning spectrometer.

The OH bands in the high resolution night airglow spectrum atlas of Broadfoot and Kendall (1968) also have been analysed for rotational temperatures. A pronounced deviation from isothermal behaviour has been found for the bands analysed (Figure 3.4). However, there is a considerable scatter in the derived rotational temperature values. This has been shown, by computer simulation, to be due principally to the spectrometer used by Broadfoot and Kendall. Although the instrument had a spectral half width of  $5\text{\AA}$ , it was used in a step-scanning mode, step  $1.2\text{\AA}$ , rather than in a continuous-scanning mode. Consequently the peak of the spectrometer

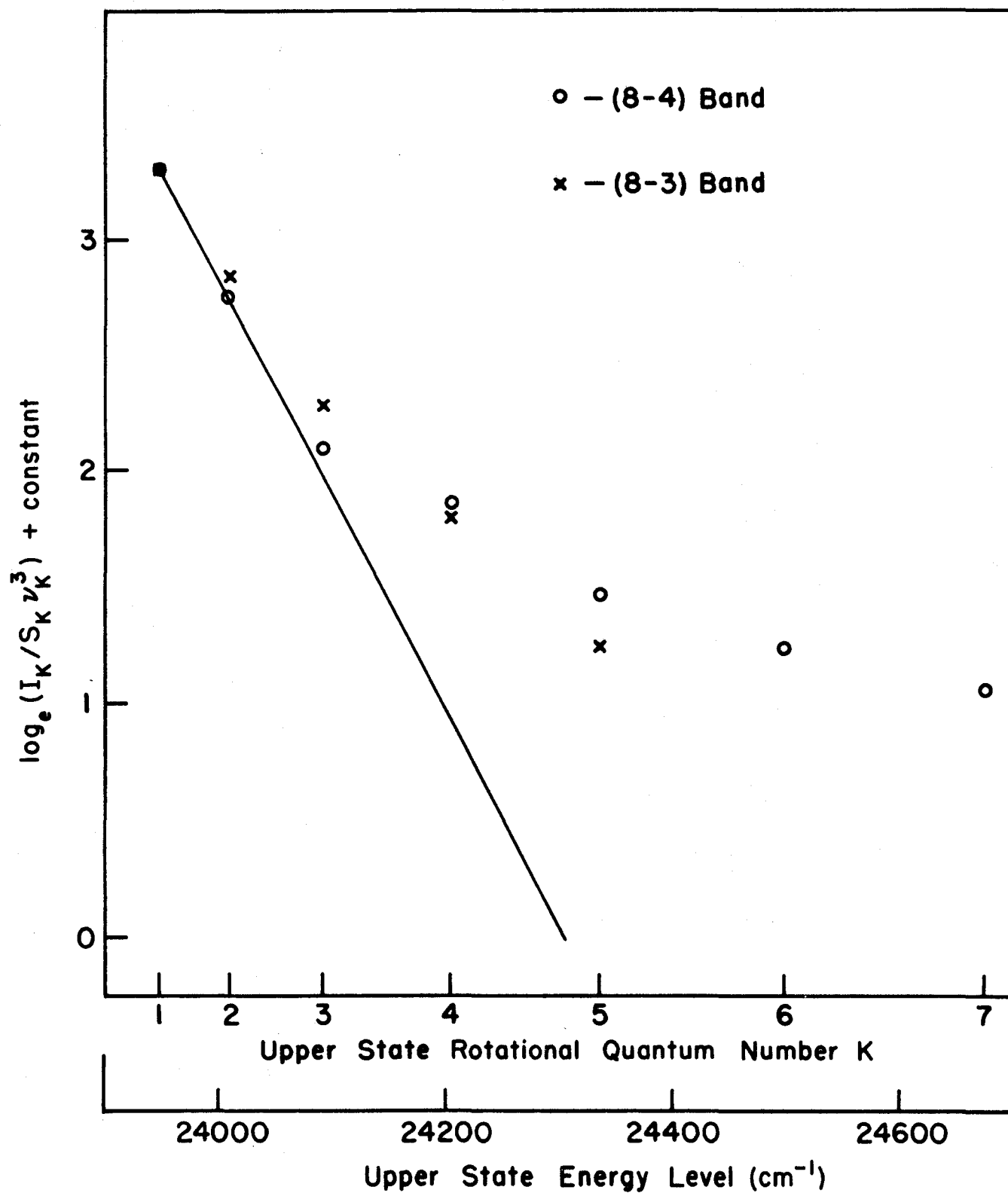


Figure 3.4: Rotational temperature graphs for observed OH(8-3) and (8-4) band spectra.

transmission function was, in general, not centered on the exact wavelength of the emission line, and small errors are therefore introduced into the intensities scaled from the published data. However, this effect is random and does not hide the non-isothermal behaviour of the rotational temperature. It also indicates that a continuous-scanning spectrometer is desirable for measurements of OH rotational spectrum from which "temperatures" are to be determined.

### 3.8.2 Photographic plates

Photographic plates are included in the category of continuous recording devices, but have the disadvantage of a nonlinear intensity response. While this does not preclude the use of photographic techniques in the determination of rotational temperatures, it is always possible that an unknown non-linearity could be introduced into the derived rotational temperatures.

The relatively recent introduction of photoelectric devices\* into high resolution OH spectrum recording may account for previous authors' failure to take notice of deviations from isothermal behaviour in the measured rotational temperature. A re-examination of previously published data obtained with photographic emulsions (McPherson and Vallance Jones, 1960; Kvifte, 1959) has shown that the non-linearities obtained by Harrison et al., (1970) are present.

---

\*Russian workers have used a combination of image intensifiers and photographic plates.

### 3.9 Discussion

The observations of Harrison et al., (1970) as confirmed by other results, have shown that there is a real deviation from isothermal rotational temperatures in the nightglow OH spectrum. The foregoing discussions have shown that in the presence of thermal equilibrium in the OH rotational populations, the only factor that introduces a significant deviation (for the bands in question) is the atmospheric temperature averaging process. However, deviations introduced by this mechanism are not sufficient for it to be the sole explanation. It must be concluded that non-equilibrium processes are important.

CHAPTER IV  
NON-ISOTHERMAL BEHAVIOUR IN OH AIRGLOW  
ROTATIONAL TEMPERATURES

2. NON-EQUILIBRIUM CONDITIONS

4.1 Introduction

It was shown in Chapter III that the assumption that rotational populations are in thermal equilibrium with the ambient atmosphere cannot provide a complete explanation of the observed features in the OH airglow spectrum. This makes it necessary to consider whether thermal equilibrium is achieved by the emitting molecules. As the Meinel OH bands are emitted over an extended height range, the collision frequency will vary considerably over the emission region (Table 4.1). For OH molecules undergoing transitions in the lower regions of the emission profile the collision frequency may permit rotational equilibrium with the surrounding atmosphere, but for molecules emitting in the upper regions there may be a significant departure from equilibrium. A comparison of the tabulated transition probabilities (Table 2.3) with the collision frequency (Table 4.1) shows that the total probability for transitions from the ninth vibrational level is equal to the collision frequency at 105 km.

If the initial rotational population distribution differs appreciably from that for thermal equilibrium, the number of collisions experienced before radiation will be important in determining the effective rotational population distribution, and spectrum, of the emitting molecules. If there are no collisions in the period between the formation of the excited OH



TABLE 4.1  
COLLISION FREQUENCY AS A FUNCTION OF HEIGHT  
(Calculated from 1966 United States  
Standard Atmosphere Data)

Ht Z(km.)	Collision Frequency $\nu(\text{sec}^{-1})$
65	$5.62 \times 10^5$
70	$2.86 \times 10^5$
75	$1.35 \times 10^5$
80	$5.79 \times 10^4$
85	$2.24 \times 10^4$
90	$8.03 \times 10^3$
95	$3.13 \times 10^3$
100	$1.19 \times 10^3$
105	$5.02 \times 10^2$
110	$2.44 \times 10^2$
115	$1.26 \times 10^2$
120	$7.65 \times 10^1$
125	$5.01 \times 10^1$
130	$3.30 \times 10^1$

states and radiative transitions, the resulting spectrum will display the rotational population distribution at the time of origin of that state. If the excited state molecules undergo some collisions before radiating, but an insufficient number to cause thermalization, the radiating population will be in an intermediate condition between the initial distribution and a thermal distribution. In order to determine this intermediate condition it is necessary to consider the possible initial populations and the probable rotational relaxation mechanism.

#### 4.2 Origin of the Initial Populations

The initial population distribution of the newly formed vibrational state will be determined by the method of formation of that state. In general, there are two ways in which a given excited state may originate. It may result either from a transition from a higher vibrational level, or it may be the state formed in the initial excitation process. In the first case the population distribution of the newly formed state will depend on the population distribution before transition, and any redistribution which may result from the transition. In the second case the population distribution will depend on the excitation mechanism. It is improbable that the newly excited rotational population distribution will be a Boltzmann distribution.

### 4.3 The Effect of Transitions on Rotational Population Distribution

#### 4.3.1 Theoretical considerations

The rotational population originating through radiative transitions from a higher vibrational level is considered for the simplest case where the emitting state population is in thermal equilibrium with the ambient medium. (Similar calculations should apply for a non-equilibrium upper state population.)

The allowed transitions which contribute to a vibration-rotation band are given by the usual rotational selection rules (for  $\Lambda = 1$ ),

$$\Delta J = -1, 0, +1 \quad (4.1)$$

and result in the P, Q, and R branches respectively. Hence, a molecule in lower rotational level  $J''$  may originate from populations in the upper rotational levels ( $J'$ ) equal to  $J'' + 1$ ,  $J''$  or  $J'' - 1$ . As the intensity (in photon units) of a spectral line is a measure of the total number of molecules that have undergone the corresponding transition, the total number of molecules in the level  $J''$  will be given by the sum of the intensities of the spectral lines from transitions into the common lower level  $J''$ . The fraction of the molecules populating a given lower rotational level  $J''$ , after transition, may be written as,

$$n(J'') = \frac{(I_p + I_q + I_r)}{\sum J} \quad (4.2)$$

where  $I_p$ ,  $I_q$ ,  $I_r$  are the intensities (in photon units) of the spectral lines involving transitions to a common lower rotational level  $J''$ , and  $\sum_J I$  is the total band intensity. The intensities of the spectral lines with a common lower level may be written as (see equation 2.22),

$$\begin{aligned}
 I_p &= \nu_p^3 S_p(J''-1) \exp\left[-\frac{E(J''-1)hc}{kT}\right] \left[\frac{C_{em}}{Q_r}\right] \\
 I_q &= \nu_q^3 S_q(J'') \exp\left[-\frac{E(J'')hc}{kT}\right] \left[\frac{C_{em}}{Q_r}\right] \\
 I_r &= \nu_r^3 S_r(J''+1) \exp\left[-\frac{E(J''+1)hc}{kT}\right] \left[\frac{C_{em}}{Q_r}\right] .
 \end{aligned} \tag{4.3}$$

From equations 4.2 and 4.3 the population in the rotational level  $J''$  may be expressed as,

$$\begin{aligned}
 n(J'') &= \left\{ \left[ \nu_p^3 S_p(J''-1) \exp\left(-\frac{E(J''-1)hc}{kT}\right) \right] + \left[ \nu_q^3 S_q(J'') \exp\left(-\frac{E(J'')hc}{kT}\right) \right] \right. \\
 &\quad \left. + \left[ \nu_r^3 S_r(J''+1) \exp\left(-\frac{E(J''+1)hc}{kT}\right) \right] \right\} / \left[ \sum_J \nu_J^3 S(J) \exp\left(-\frac{E(J)hc}{kT}\right) \right] .
 \end{aligned} \tag{4.4}$$

The wave numbers  $\nu$  are approximately constant for all the lines in the band, so that equation 4.4 may be simplified as follows, to give:

$$n(J'') = \left\{ [S_p(J''-1) \exp(\frac{-E(J''-1)hc}{kT})] + [S_q(J'') \exp(\frac{-E(J'')hc}{kT})] + [S_r(J''+1) \exp(\frac{-E(J''+1)hc}{kT})] \right\} / [\sum_J S(J) \exp(\frac{-E(J)hc}{kT})] \quad (4.5)$$

If the lower state population is in thermal equilibrium at temperature  $T$ , then the fractional population of rotational level  $J''$  may be written, according to the Boltzmann expression, (Herzberg, 1950),

$$n(J'') = [(2J''+1) \exp(\frac{-E(J'')hc}{kT})] / [\sum_J (2J+1) \exp(\frac{-E(J)hc}{kT})] \quad (4.6)$$

A comparison of equations 4.5 and 4.6 shows that the equilibrium rotational population of the upper level has been redistributed by transitions to give a different (and therefore non-equilibrium) rotational distribution.

#### 4.3.2 The variation of the transition effect for different bands

The total energy of a state may be written as the sum of its rotational and vibrational terms,

$$E(v, J) = G(v) + F_v(J) \quad (4.7)$$

where  $E(v, J)$  is the total energy of the state,  $G(v)$  is the vibrational term, and  $F_v(J)$  is the rotational term. For a given band  $G(v)$  is constant and it follows from equation 4.5 that,

$$n(J'') = \left\{ [S_p(J''-1) \exp(\frac{-F_v(J''-1)hc}{kT})] + [S_q(J'') \exp(\frac{-F_v(J'')hc}{kT})] + [S_r(J''+1) \exp(\frac{-F_v(J''+1)hc}{kT})] \right\} / \left[ \sum_J S(J) \exp(\frac{-F_v(J)hc}{kT}) \right]. \quad (4.8)$$

This expression is independent of the vibrational term energy, and the only dependence on the vibrational level is that of the rotational term energy. To a good approximation the rotational term energy may be written,

$$F_v(J) = B_v J(J+1) \quad (4.9)$$

where  $B_v$  is the rotational constant for the vibrational level  $v$ , and may be written as (Herzberg, 1950),

$$B_v = B_e - \alpha_e(v+1/2) \quad (4.10)$$

where  $B_e$  and  $\alpha_e$  are constants for the molecule. For ground state OH molecules  $B_v$  varies between  $18.515 \text{ cm}^{-1}$  for  $v = 0$  and  $12.33 \text{ cm}^{-1}$  for  $v = 9$ . Hence, there is a definite vibrational level dependence in the equation for  $n(J'')$ , so that the transition effect will in general depend on the upper vibrational level.

#### 4.3.3 Quantitative calculation of the transition effect

Numerical calculations using equation 4.4 have shown that the lower state rotational population is approximately described by an isothermal (Boltzmann) distribution, but corresponding to a higher temperature than the initial equilibrium temperature. The lower state rotational population

distribution for the (7-3) band expressed in terms of rotational temperatures\* is given in Table 4.2, for a range of initial equilibrium temperatures. This population may now become the upper state population for a new radiative transition, although there is a possibility of collisional redistribution. If the distribution is not affected by thermalizing collisions, the rotational temperature determined from the resulting spectra (bands with  $v' = 3$ ) will be the rotational population temperature given in Table 4.2.

This effect has also been considered in a simplified manner by Wallace (1961). For a sequence of vibrational transitions with  $\Delta v = 1$ , and neglecting collisions, Wallace showed that there would be an increasing accumulation of population in the higher rotational levels with decreasing vibrational level  $v$ . This population enhancement would give an increasing rotational temperature for bands with decreasing upper vibrational level  $v'$ . The absence of any strong effect of this nature in observed spectra was taken to indicate that the radiating molecules are re-thermalized following each transition.

#### 4.4 Partial Thermalization in Non-Equilibrium Populations

##### 4.4.1 Introduction

In the previous discussion it was assumed that the excited molecules do not suffer thermalizing collisions during their radiative lifetime. This assumption was made to clarify the role of the processes being discussed.

---

\*These "temperatures" are defined in a similar manner to the rotational "temperatures" in Chapter 3, but using the ratio of Boltzmann populations (Equation 4.6) instead of the ratio of the line intensities.

TABLE 4.2  
 TRANSITION EFFECT, (7-3) BAND  
 (Rotational Population Temperatures of Lower State,  
 for a Range of Upper State Equilibrium Temperatures,  $T_{EQ}$  ( $^{\circ}K$ ).)

$T_{EQ}$	$T_{23}$	$T_{24}$	$T_{25}$	$T_{26}$	$T_{27}$	$T_{28}$	$T_{29}$	$T_{210}$
200	295.8	295.7	291.5	288.4	285.4	282.6	280.0	277.5
300	414.2	415.5	411.7	410.1	408.3	406.6	405.0	403.2
400	536.5	557.5	532.7	531.3	529.8	528.6	527.5	526.2
500	661.7	661.3	654.6	652.9	651.4	650.2	649.4	648.3
600	789.2	786.5	777.4	775.2	773.3	771.9	771.2	770.1



In practice there will be a number of collisions between the excited OH molecules and the ambient atmospheric molecules before the radiative transition. The exact number of collisions is determined by the atmospheric collision frequency, at the altitude in question, and the radiative lifetime. If the collision frequency is smaller than the transition probability -- i.e. if the time between collisions is longer than the radiative lifetime -- the rotational spectrum will exhibit the population distribution occurring at the time of origin of the excited states. If the time between collisions is shorter by some orders of magnitude than the radiative lifetime the rotational population will be nearly thermalized. In the latter case the derived rotational temperature will be very close to the ambient gas kinetic temperature.

In order to determine the population distribution for intermediate cases -- i.e. where the radiative lifetime is of the same order as the collision time -- it is necessary to know the mechanism by which energy is lost in collisions, and the initial rotational population distribution. It is then possible to describe the state of the system at any time in terms of a relaxation process.

#### 4.4.2 Relaxation processes

To understand the effects of relaxation processes it is convenient to consider a simple case first. In this model it is assumed firstly that the initial excited population has a Boltzmann distribution at a temperature  $T'$ , which is higher than the equilibrium temperature  $T_0$ , and secondly that the

excited molecules lose one-half of their excess energy per collision. An "average" molecule will initially have an excess rotational energy  $k(T'-T_0)$ , and the "half energy loss" model requires it to lose energy  $1/2k(T'-T_0)$  in its first collision,  $1/4k(T'-T_0)$  in the second collision, and so on.

Since the energy loss is expressed in terms of temperature the excited population can at all times be characterized by a temperature. This is a reasonable assumption, as more complex relaxation calculations indicate that a "hot" Boltzmann distribution does relax through a series of distributions which are approximately Boltzmann (i.e. can be described by a 'temperature') (Herman and Shuler, 1958).

The temperature of the excited molecules may be expressed as a function of time,

$$T(t) = \frac{T_0 + (T'-T_0)}{2^{n(t)}} \quad (4.11)$$

where each molecule has experienced  $n$  collisions in the time  $t$  since formation. Equation 4.11 may be rewritten in terms of the collision frequency,  $\nu$ ,

$$n(t) = \nu t \quad (4.12)$$

so

$$T(t) = \frac{T_0 + (T'-T_0)}{2^{\nu t}}, \quad (4.13)$$

or

$$T(t) = T_0 + (T'-T_0) \exp(-\nu \log_e 2 \cdot t) \quad (4.14)$$

The "half energy loss" model may be seen to be a relaxation process by considering the usual relaxation equation,

$$\frac{dT(t)}{dt} = - \frac{1}{\tau_R} (T(t) - T_0) \quad (4.15)$$

where  $\tau_R$  is the "relaxation time" (Raff and Winter, 1968).

Equation 4.15 has the solution,

$$T(t) = T_0 + (T(0) - T_0) \exp\left(-\frac{t}{\tau_R}\right) \quad (4.16)$$

and the two solutions 4.14 and 4.16 are identical when,

$$\tau_R = \frac{1}{\nu \log_e 2} \quad (4.17)$$

It should be noted that the latter description is independent of any explicit energy loss mechanism; it is the choice of such a mechanism that determines the value of  $\tau_R$ .

#### 4.4.3 Simple relaxation with radiative loss mechanisms

As the OH molecules are radiating while the rotational distribution is relaxing, there are more radiating molecules when the population is "hot" than when it has thermalized. Therefore, the rotational temperature determined from the emission spectrum will be weighted in favour of the hotter population. If it is assumed that the population may be described at all times by a Boltzmann distribution, and thus a temperature, the mean rotational temperature during the relaxation is given by,

$$\bar{T}_R = \frac{\int_0^{\infty} N(t)T(t)dt}{\int_0^{\infty} N(t)dt} \quad (4.18)$$

where  $N(t)$  is the number of excited molecules and  $T(t)$  is the Boltzmann temperature of the relaxing population.

The number of excited molecules at a time  $t$  is,

$$N(t) = N_0 \exp(-At) \quad (4.19)$$

where  $N_0$  is the initial excited population and  $A$  is the total transition probability, for the bands through which the excited population is decaying. If the values of  $N(t)$  and  $T(t)$  from equations 4.19 and 4.16 are substituted into equation 4.18 then,

$$\bar{T}_R = \frac{\int_0^{\infty} N_0 \exp(-At) [T_0 + (T(0) - T_0) \exp(\frac{-t}{\tau_R})] dt}{\int_0^{\infty} N_0 \exp(-At) dt} \quad (4.20)$$

which simplifies to,

$$\bar{T}_R = \frac{T_0 + (T(0) - T_0)}{1 + \frac{1}{A\tau_R}} \quad (4.21)$$

This is the value of the rotational temperature that would be determined from the emission spectrum for an excited population relaxing through a series of Boltzmann distributions with relaxation time  $\tau_R$ .

#### 4.4.4 Discussion of the simple model

The "half energy loss" model provides some indication of the relaxation of a rotational population and has been used to describe the relaxation of "hot" Boltzmann distributions such as occur after vibration-rotation transitions from thermalized levels, (Section 4.3). It cannot be used to describe the relaxation of initial population distributions which are not Boltzmann.

In this model it is assumed that rotational energy may be transferred in collisions in any amount, and the discrete nature of the rotational energy levels is neglected. This assumption is valid only if the energy spacing between adjacent rotational levels is much less than the mean thermal energy of the molecules. From equation 4.9 this requirement may be written as,

$$2B_v(J+1) \ll 3/2kT \quad (4.22)$$

and for average values in the OH molecule this requires  $T \sim 1500^\circ\text{K}$ , which is significantly greater than the atmospheric temperature in the emission region.

It is also assumed that the relaxation may be described in terms of a single relaxation time  $\tau_R$ , as defined in equation 4.15. Shuler (1959) has shown that for a system with more than two energy levels it may not be possible to characterize the relaxation by a single relaxation time.

For these reasons, a more complicated model has been considered which takes into account the quantum nature of the rotational energy, and permits the discussion of relaxation for initial distributions which are not Boltzmann.

## 4.5 Weak Interaction Relaxation Theory

### 4.5.1 Introduction

A number of authors have considered the problem of vibrational and rotational relaxation of excited diatomic molecule populations (Clarke and McChesney, 1964). The relaxation has in all cases been described in terms of a weak interaction between rotational and kinetic energies. It is possible that a weak interaction may not describe the rotational relaxation for OH, as will be discussed later, but in the absence of other information a weak interaction model has been assumed.

### 4.5.2 Rotational relaxation

For a non-radiating thermodynamic system with discrete energy levels characterized by quantum numbers I, J etc., the rate of change of population in the  $J^{\text{th}}$  level is given by,

$$\frac{dn_J}{dt} = \sum_{\substack{I \\ I \neq J}} K_{JI} n_I(t) - \sum_{\substack{I \\ I \neq J}} K_{IJ} n_J(t) \quad (4.23)$$

where  $K_{JI}$  is the probability for a transition from level I to level J,  $K_{IJ}$  is the probability for the reverse transition, and  $n_J(t)$  and  $n_I(t)$  are the populations of the  $J^{\text{th}}$  and  $I^{\text{th}}$  levels respectively. The first term on the right-hand side of equation 4.23 is the population gain by level J from other levels, and the second term is the population loss from level J to the other levels.

Equation 4.23 may be applied to the collisional relaxation of vibrationally or rotationally excited molecules

immersed in a "bath" of thermalized particles. In this case  $K_{JI}$  may be written,

$$K_{JI} = ZQ_{JI}N_{I,J} \quad (4.24)$$

where  $Z$  is the collision frequency per unit oscillator density,  $Q_{JI}$  is the transition probability per collision, and  $N_{I,J}$  is the fraction of "bath" particles with sufficient energy to excite a molecule from level  $I$  to level  $J$ . Similarly  $K_{IJ}$  is given by,

$$K_{IJ} = ZQ_{IJ}N_{J,I} \quad (4.25)$$

Herman and Shuler (1958) have considered the problem of the simultaneous vibrational and rotational relaxation of an excited diatomic species, and have shown that to a very good approximation, the rotation and vibration modes relax independently. This is due to the time scales for each relaxation: the rotational mode relaxes between  $10^2$  and  $10^5$  times faster than the vibrational mode. The rotational relaxation may, therefore, be considered independently of the vibrational relaxation.

For the weak interaction theory of rotational relaxation proposed by Takayanagi (1952) and Brout (1954), the collisional rotation transition selection rules are the same as for optical transitions. For the case where  $\Lambda = 1$  ( $\Pi$  electronic states), these are,

$$\Delta J = -1, 0, +1 \quad (4.26)$$

Similarly, the collisional rotation transition probabilities are proportional to the optical transition probabilities.

The probabilities for collisional rotational transitions between levels  $J+1$ ,  $J$ , and  $J-1$ , for a rigid rotator, may be written,

$$\begin{aligned}
 Q_{J,J+1} &= \left[ \frac{(J+1+\Omega)(J+1-\Omega)}{J+1} \right] \left[ \frac{Q_{10}}{2J+1} \right] \\
 Q_{J,J} &= \left[ \frac{(2J+1)\Omega^2}{J(J+1)} \right] \left[ \frac{Q_{10}}{2J+1} \right] \\
 Q_{J,J-1} &= \left[ \frac{(J+\Omega)(J-\Omega)}{J} \right] \left[ \frac{Q_{10}}{2J+1} \right] \quad (4.27)
 \end{aligned}$$

where  $\Omega = 3/2, 1/2$  for the two spin multiplets of OH.  $Q_{10}$  is the collision transition probability between the two lowest  $J$  levels, and is a measure of the probability that a collision will cause a rotational transition. If the selection rules given in equation 4.26 apply, then the only non-zero rotational transition probabilities for the level  $J$  are given by equation 4.27, and correspond to the P, Q, and R branches in optical transitions.

The collisional transition probabilities  $Q$  may be expressed in terms of the relevant optical line strengths:

$$\begin{aligned}
 Q_{J,J+1} &= [S_P(J)] \left[ \frac{Q_{10}}{2J+1} \right] \\
 Q_{J,J} &= [S_Q(J)] \left[ \frac{Q_{10}}{2J+1} \right] \\
 Q_{J,J-1} &= [S_R(J)] \left[ \frac{Q_{10}}{2J+1} \right] \quad (4.28)
 \end{aligned}$$

If it is assumed that the vibrational relaxation may be



neglected, the equation (4.23) for collisional relaxation of the rotational population may be written as,

$$\begin{aligned} \frac{1}{Q_{10}Z} \frac{dn_J}{dt} = & \left[ \frac{S_R(J+1)n_{J+1}N_{J+1,J}}{2J+3} \right] - \left[ \frac{S_P(J)n_JN_{J,J+1}}{2J+1} \right] \\ & + \left[ \frac{S_P(J-1)n_{J-1}N_{J-1,J}}{2J-1} \right] - \left[ \frac{S_R(J)n_JN_{J,J-1}}{2J+1} \right] . \end{aligned} \quad (4.29)$$

In general, any bath particle is capable of causing de-excitation, so that,

$$N_{J+1,J} = N_{J,J-1} = N \quad (4.30)$$

where  $N$  is the total number of bath particles. Also,

$$\begin{aligned} S_R(J+1) &= S_P(J) \\ S_R(J) &= S_P(J-1) \end{aligned} \quad (4.31)$$

and hence equation 4.29 becomes,

$$\begin{aligned} \frac{1}{Q_{10}Z} \frac{dn_J}{dt} = & [S_P(J)] \left[ \frac{n_{J+1}N}{2J+3} - \frac{n_JN_{J,J+1}}{2J+1} \right] \\ & + [S_R(J)] \left[ \frac{n_{J-1}N_{J-1,J}}{2J-1} - \frac{n_JN}{2J+1} \right] . \end{aligned} \quad (4.32)$$

From the principle of detailed balance, each set of brackets in equation 4.32 must be separately equal to zero at equilibrium. Hence, if the equilibrium populations for levels  $J$ ,  $J+1$ ,  $J-1$  are written  $\bar{n}_J$ ,  $\bar{n}_{J+1}$ ,  $\bar{n}_{J-1}$ , then,

$$\frac{\bar{n}_{J+1}}{\bar{n}_J} = \frac{N_{J,J+1} (2J+3)}{N (2J+1)}$$

and

$$\frac{\bar{n}_{J-1}}{\bar{n}_J} = \frac{N (2J-1)}{N_{J-1,J} (2J+1)} \quad (4.33)$$

These equilibrium populations are also given by Boltzmann distributions:

$$\bar{n}_J = \frac{(2J+1) \exp\left[-\frac{J(J+1)B}{kT}\right]}{\sum_J (2J+1) \exp\left[-\frac{J(J+1)B}{kT}\right]} \quad (4.34)$$

It follows that,

$$\frac{\bar{n}_{J+1}}{\bar{n}_J} = \frac{(2J+3) \exp\left[-\frac{(J+1)(J+2)B}{kT}\right]}{(2J+1) \exp\left[-\frac{J(J+1)B}{kT}\right]}$$

and,

$$\frac{\bar{n}_{J-1}}{\bar{n}_J} = \frac{(2J-1) \exp\left[-\frac{J(J-1)B}{kT}\right]}{(2J+1) \exp\left[-\frac{J(J+1)B}{kT}\right]} \quad (4.35)$$

From equations 4.33 and 4.35,

$$N_{J,J+1} = N \exp[-2(J+1)\Psi] \quad (4.36)$$

and

$$N_{J-1,J} = N \exp(-2J\Psi) \quad (4.37)$$

where,

$$\Psi = \frac{B}{kT} \quad . \quad (4.38)$$

As the collision frequency  $\nu$  may be written in terms of  $Z$ , the collision frequency per unit oscillator density, and  $N$ , the number density of bath particles,

$$NZ = \nu \quad , \quad (4.39)$$

the rotational relaxation equation (4.32) may be written,

$$\begin{aligned} \frac{1}{Q_{10}\nu} \frac{dn_J}{dt} = & [n_{J+1} \left( \frac{S_P(J)}{2J+3} \right)] + [n_{J-1} \left( \frac{S_R(J)}{2J-1} \right) \exp(-2J\Psi)] \\ & - [n_J \left( \frac{S_P(J) \exp(-2(J+1)\Psi)}{(2J+1)} + \frac{S_R(J)}{(2J+1)} \right)] \quad . \end{aligned} \quad (4.40)$$

#### 4.5.3 Solution of the relaxation equation.

Herman and Shuler (1958) have found no simple analytic solution to equations such as 4.40. Satisfactory numerical solutions may be obtained from a Taylor expansion (Wilkes, 1966) of the form,

$$n_J(t) = n_J(t_0) - (t-t_0)n'_J + \frac{(t-t_0)^2}{2} n''_J(t_0) \quad (4.41)$$

with the time interval,

$$(t-t_0) = \frac{0.1}{\nu} \quad , \quad (4.42)$$

where  $\nu$  is the collision frequency. The method has been found

to be accurate for time intervals between  $.01/\nu$  and  $1/\nu$ , and may be used to determine the rotational relaxation for any initial population  $[n_j(t=0)]$ .

Herman and Shuler (1958) have shown from calculations similar to the above that a "hot" Boltzmann distribution will relax through a series of nearly isothermal distributions. This is in agreement with the simple "half energy loss" model (section 4.4).

To investigate the relaxation of an initial population confined to a single rotational level calculations have been made for the OH molecule with an initial population in the ninth vibrational level and the seventh rotational level. The initial conditions for equation 4.40 may be written as,

$$\begin{aligned} n_j(0) &= 1, & J &= \frac{15}{2} & (K=7) \\ &= 0, & J &\neq \frac{15}{2} & (K \neq 7) \end{aligned} \quad (4.43)$$

It was found that at a "bath" temperature of 500°K, the population had relaxed to within 1% of an equilibrium Boltzmann distribution after 72 collisions, and for a "bath" temperature of 165°K after 48 collisions.

This temperature dependence may be understood from equation 4.40. The exponential terms correspond to collisions increasing the rotational quantum number. The magnitude of these terms increases with temperature. Physically, this means that for higher temperatures there are more bath particles

capable of exciting the relaxing molecules, and "cooling" will be retarded.

The population distributions for various times during the relaxation process are shown in Figure 4.1.

#### 4.5.4 Radiative relaxation.

The weak interaction model discussions have neglected the possibility of radiation during the collisional relaxation. The collisionally relaxing population is being depleted continuously by radiation. If the rotational population of the level  $J$  which is undergoing collisional relaxation, as determined by equation 4.40, is  $n_J(t)$ , the true population  $N_J(t)$  of level  $J$  as a function of time, with radiative losses included, may be written,

$$N_J(t) = n_J(t) \exp(-At) \quad (4.44)$$

where  $A$  is the total optical vibrational transition probability and  $t$  is the time since the formation of the excited vibrational level. The number of molecules that radiate in the time interval  $t$  to  $t+\delta t$  is given by,

$$\delta N_J = -n_J(t) A \exp(-At) \delta t \quad (4.45)$$

The intensity of an emission line is proportional to the total number of molecules that radiate through the relevant transition. Hence, the emitted spectrum may be determined from the "effective population",  $\bar{N}_J$ , which is determined by the summation of  $\delta N_J$  for all time intervals  $\delta t$ ,

$$\bar{N}_J = A \sum_{i=1}^{\infty} n_J(t_i) \exp(-At_i) \delta t \quad (4.46)$$

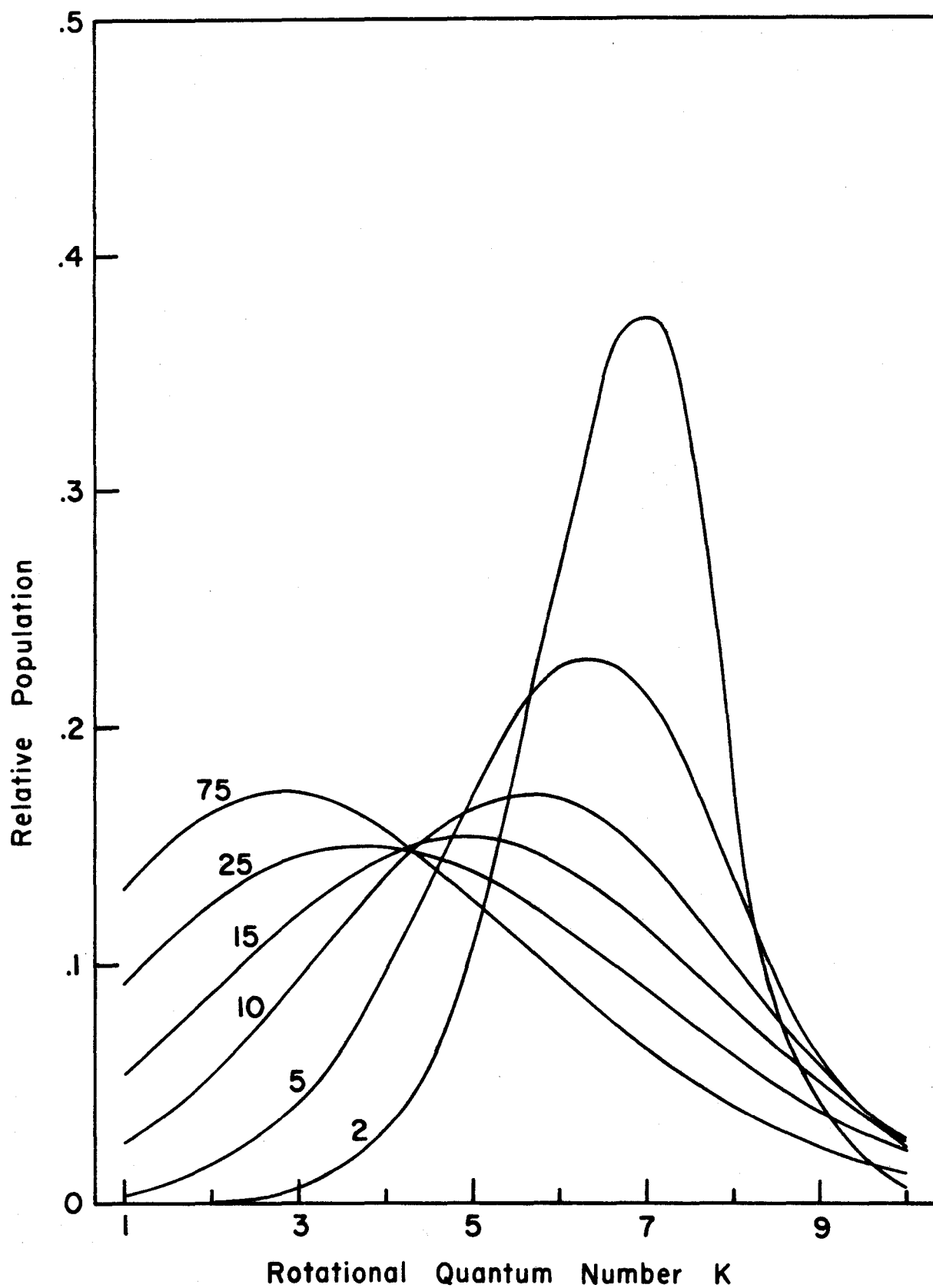


Figure 4.1: Rotational relaxation in a non-radiating population. (Time units in terms of  $1/\nu_{\text{coll}}$ .)

As the population is decaying through radiation it is only necessary to continue the summation until the exponential term has become very small. Computer calculations have shown that continuing the summation beyond 20 radiative lifetimes does not appreciably change the effective emitting population  $\bar{N}_J$  for any value of  $J$ .

For an initial population distribution restricted to a single rotational level, the form of the emitted spectrum is strongly dependent on the relative values of the time between collisions,  $1/\nu$ , and the radiative lifetime,  $1/A$ . If the time between collisions is very much shorter than the radiative lifetime, the emitted spectrum will be approximately a thermal spectrum (isothermal rotational temperatures). As the maximum rate of radiative loss occurs at  $t = 0$ , the collisional relaxation must proceed rapidly, relative to  $1/A$ , in order to achieve a nearly thermal spectrum. For the situation where the radiative lifetime is shorter than the time between collisions, the emitted spectrum will be extremely non-thermal, and will be determined almost entirely by the initial excited population distribution.

To achieve the required accuracy in the calculations, the integration time interval, in the numerical solution of the relaxation equations including radiation, has been taken as the smaller of the values  $0.1/\nu$  and  $0.1/A$ .

Figure 4.2 shows the effective population for the cases where  $\nu = 0.1A$ ,  $\nu = A$ , and  $\nu = 10A$ , at a "bath" temperature of  $500^\circ\text{K}$ . For comparison a Boltzmann population distribution for the same temperature is shown.

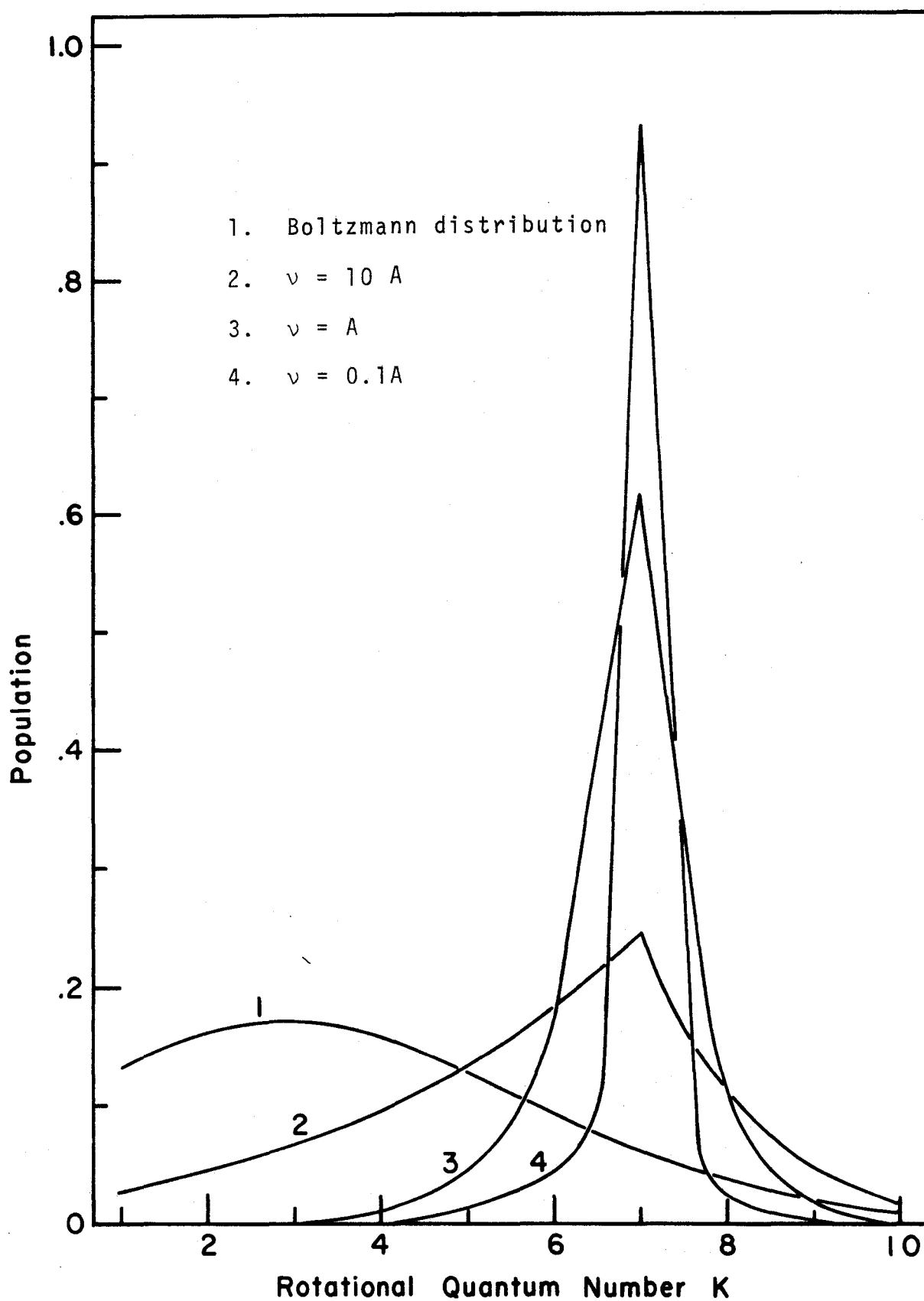


Figure 4.2: Effective Population distribution for different ratios of collision frequency and transition probability.



#### 4.6 Applicability of Weak Interaction Theory to Rotational Relaxation Processes

If the interaction during collisions between kinetic and rotational energy is to be weak, Ehrenfest's Adiabatic Principle requires that the interaction time be considerably greater than the rotation period. This may be written (Clarke and McChesney, 1964),

$$\frac{s}{V} > \frac{1}{\nu_{ROT}} \quad (4.47)$$

where  $s$  is the interaction distance,  $V$  is the thermal molecular speed, and  $1/\nu_{ROT}$  is the rotational period. To evaluate this inequality, the most probable velocity may be substituted for  $V$ , and the equilibrium internuclear separation,  $r_e$ , for  $s$ . If the rotational period is expressed in terms of the rotational energy ( $E_{ROT}$ ), equation 4.47 may be written,

$$r_e / \sqrt{\frac{2kT}{\mu}} > \frac{h}{E_{ROT}} \quad (4.48)$$

where  $\mu$  is the reduced mass of the collision pair and  $T$  is the gas kinetic temperature. For the case where the colliding molecules are OH and  $O_2$ , at an ambient temperature of  $200^\circ K$ , the requirement for the interaction to be weak reduces to,

$$E_{ROT} > 180 \text{ cm}^{-1} * \quad (4.49)$$

---

\*See footnote, page 8.

The energy difference between the first two rotational levels of the first vibrational level of  $\text{OH}(^2\Pi)$ , which may be taken as a measure of  $E_{\text{ROT}}$ , is approximately  $80 \text{ cm}^{-1}$  (Dieke and Crosswhite, 1948). Therefore, the adiabatic inequality is not satisfied for the OH molecule, and the weak interaction theory does not strictly hold.

For the molecules  $\text{O}_2$  and  $\text{N}_2$  the adiabatic inequality also does not hold. The agreement is far worse than for the OH molecule, as the energy spacing of the lowest rotational levels is approximately  $3 \text{ cm}^{-1}$ . Experimental evidence (Herman and Shuler, 1958) indicates that the true "relaxation times" for  $\text{O}_2$  and  $\text{N}_2$  are shorter by a factor of  $10^2$  than the value predicted by the weak interaction theory\*. For  $\text{H}_2$  and  $\text{D}_2$ , in which the rotational energy spacing is large, the experimental values for the relaxation time are in agreement with the weak interaction theory results.

The value of the rotational constant  $B_v$  determines the spacing of the rotational energy levels (c.f. equation 4.9) and will therefore be a measure of the validity of the adiabatic inequality. The OH molecule is intermediate in  $B_v$  value between molecules for which the weak interaction theory gives correct results and molecules for which it does not. Since the  $B_v$  value for OH ( $\sim 15 \text{ cm}^{-1}$ ) is closer in magnitude to that

---

\*"Relaxation time" is defined here as the time which is taken for an excited population to relax to where the rotational energy difference from an equilibrium distribution has decreased to  $1/e$  of its initial value.

for  $\text{H}_2$  ( $\sim 60 \text{ cm}^{-1}$ ) than to that for  $\text{O}_2$  ( $\sim 1.4 \text{ cm}^{-1}$ ), it is reasonable to assume that the weak interaction theory gives a good first order description of the rotational relaxation of OH.

## CHAPTER V

### APPLICATION OF RELAXATION PROCESSES TO THE AIRGLOW EMISSIONS

#### 5.1 Excitation Mechanisms for the OH Airglow

##### 5.1.1 Introduction

To calculate the OH airglow spectrum that is observed from the ground, it is necessary to know the temperature, collision frequency, and OH volume emission rate as functions of height, and the initial population distribution of the excited OH molecules. The atmospheric temperatures and collision frequencies for this work have been taken from the United States Standard Atmosphere (1966) tables. The volume emission rate has been derived from experimental observations of the emission height profile (c.f. §3.2).

For the calculations discussed in §4.5 it was assumed that the initial OH population was confined to a single rotational level. If the relaxation calculations are to be applied to the atmospheric OH emissions the true initial population distribution must be determined for the probable excitation mechanism(s).

##### 5.1.2 Hydrogen-Ozone reaction

It is generally accepted that the major source of excited atmospheric OH molecules is the reaction between ozone and atomic hydrogen:\*

---

\* A number of other reactions have been suggested as contributory to the atmospheric OH populations, but there is no general agreement as to their importance (Breig, 1970).



(Bates and Nicolet, 1950; Nicolet, 1970). If all the energy available from this reaction is absorbed by the OH molecule, excitation into the ninth vibrational level is possible.

The fraction of the total energy that is available for exciting the internal energy modes of the OH molecule (rotation and vibration) is uncertain. Polanyi (1959) and Norrish (1964) have shown that in exothermic reactions of the type,



the major part of the reaction energy will go into vibrational excitation of the newly formed bond. In the ozone-hydrogen reaction, the newly formed OH molecule should therefore be excited into the highest available vibrational levels ( $v \leq 9$ ). However, Chamberlain and Smith (1959) have shown that the airglow OH molecules must be formed in all vibrational levels up to  $v = 9$ , to explain the observed nightglow OH band intensities. This conclusion may be incorrect, as the observational data used was not extensive and the effect of vibrational relaxation by collisions was neglected. Anlauf et al. (1968) have studied the ozone-hydrogen reaction in the laboratory, and have shown that the OH molecules are formed principally in the eighth and ninth vibrational levels. This has been confirmed in other laboratory investigations (Velculesu, 1970), which indicate that the OH molecules are formed only in the eighth and ninth vibrational levels.

### 5.1.3 Rotational level populations.

The heat of reaction for the ozone-hydrogen reaction is 77.10 kcal. per mole (or  $26969\text{cm}^{-1}$ )(Kaufman, 1964), which does not correspond exactly with any of the available rotation-vibration energy levels in the OH molecule (Table 5.1). Excitation into rotational levels different in energy from the heat of reaction may be explained by contribution from the kinetic energy of the reacting species. Polanyi (1959) has shown that the kinetic energy of the reacting species ( $\text{O}_3, \text{H}$ ) may contribute to the rotational-vibrational excitation in the new bond (OH). However, if the products are to separate after the reaction, not all the available kinetic energy may be absorbed by the OH bond.

The upper limit to the internal energy of the new bond is given by the sum of the heat of reaction and the kinetic energies of the reacting species. This may be written, for average molecules,

$$E_{\text{OH}} < \Delta H + 3kT \quad (5.3)$$

where  $E_{\text{OH}}$  is the energy of a possible excited rotational-vibrational level,  $\Delta H$  is the heat of reaction, and  $T$  is the kinetic temperature of the reacting species.

The laboratory ozone-hydrogen reaction experiments have not shown any significant gas heating, which indicates that there is no net direct contribution to the kinetic energies of the reaction products from the heat of reaction. This imposes a lower limit to the energy of the possible excited rotation-

vibration levels in the OH molecule and it may be assumed, for average reacting species that,

$$E_{OH} \geq \Delta H - 3kT \quad (5.4)$$

(This condition is valid only if the kinetic energies of the reaction products are thermal.)

The rotation-vibration energy levels given in Table 5.1 are those which satisfy the above conditions, for a kinetic temperature  $T = 200^\circ\text{K}$ . It is evident that there are suitable energy levels available for all vibrational levels ( $v' \leq 9$ ) to be excited. The results of Anlauf *et al.* (1968) and Velculescu (1970) suggest significant excitation into the eighth and ninth vibrational levels only. The apparent absence of excitation to lower levels may be explained if either the reaction kinetics do not permit the excitation of energetic rotational levels (low  $v'$ ), or excitation to the lower vibrational levels is restricted by the scarcity of suitable rotational levels (see Table 5.1).

#### 5.1.4 Spin doublet level populations.

The energy levels available suggest that both spin doublet levels are populated appreciably, although the exact ratio of population rates cannot be determined without the precise value of the heat of reaction,  $\Delta H$ , and a knowledge of the role of kinetic energy in the excitation.\*

---

\*Evidence has been found for collisional transitions violating the spin selection rule ( $\Delta\Sigma=0$ ) in the relaxation of CN (Evenson and Broida, 1966), NO (Bauer *et al.*, 1959) and OH( $^2\Sigma^+$ ) at high temperatures (Carrington, 1959). However, in each of these cases, weak interaction theory is not applicable.

TABLE 5.1

OH ENERGY LEVELS NEAR THE REACTION ENERGY, ( $26969\text{ cm}^{-1}$ )

Vibrational Level (v)	Rotational Level (K)	Spin Doublet Line	Energy ( $\text{cm}^{-1}$ )
9	5	1	26546
		2	26623
	6	1	26693
		2	26763
	7	1	26864
		2	26926
	8	1	27057
		2	27113
	9	1	27271
		2	27323
8	14	1	26598
		2	26633
	15	1	26962
		2	26995
	16	1	27346
		2	27377
7	20	1	26982
		2	27005
6	24	1	26931
		2	26950
5	27	1	26587
		2	26604
	28	1	27275
		2	27291
4	31	1	27172
		2	27186
3	34	1	27213
		2	27226
2	36	1	26548
		2	26560
1	39	1	26935
		2	26945



Spin doublet temperatures (c.f. Chapter II) have been determined from nightglow OH spectra by Meinel (1950) and Blackwell et al. (1960), which may be compared with the rotational "temperatures" determined from the same spectra. Although neither "temperature" will correspond exactly to a kinetic temperature, the relative magnitudes should be a measure of the population rates into the doublet levels. In both cases, the spin doublet temperatures are lower than the rotational temperatures by  $\sim 70^\circ\text{K}$ . This suggests that the  $^2\Pi_{1/2}$  levels are underpopulated relative to the  $^2\Pi_{3/2}$  levels.

#### 5.1.5 Initial populations in airglow calculations.

From the foregoing discussions it is apparent that the details of the ozone-hydrogen excitation mechanism for OH are not well known. Experimental evidence suggests that all the reaction energy goes into the newly formed bond and that the OH molecules are formed in the eighth and ninth vibrational levels with rotation-vibration energies close to the heat of reaction (Anlauf et al., 1968).

In the absence of a more accurate knowledge of the initial population distribution, a simple distribution has been considered for the OH airglow calculations. It is assumed that the OH molecules are formed only in levels ( $v=9$ ,  $K=7$ ) and ( $v=8$ ,  $K=15$ ). The ratio of formation in these levels is taken as  $N(v=8): N(v=9) = 1:4$ , in agreement with experimental data (Velculescu, 1970).

Relaxation in the  $^2\Pi_{1/2}$  spin doublet levels has been

neglected in the calculations of the  ${}^2\Pi_{3/2}$  airglow spectra, as the populations of the two sets of levels relax independently for weak interaction theory.

## 5.2 Calculation of the OH Airglow Spectrum by the Weak Interaction Relaxation Process.

### 5.2.1 Calculation of ground based spectra.

The OH airglow spectrum observed from the ground is determined by the total "effective population" for the atmosphere, which is the sum over all heights of the local "effective populations".

The fraction of the local effective population at height  $z$  in the  $K^{\text{th}}$  rotational level (in a given vibrational level)  $\bar{N}_K(z)$ , may be determined from the relaxation equation (4.40). If the volume emission rate at height  $z$  is  $P(z)$ , then the local effective population in rotational level  $K$  at height  $z$  is  $\bar{N}_K(z) P(z)$ . The total atmospheric effective population in level  $K$  is therefore,

$$\bar{N}_K(\text{total}) = \int_{z_1}^{z_2} \bar{N}_K(z) P(z) dz \quad (5.5)$$

where  $z_1$  and  $z_2$  are the lower and upper altitude limits of the OH emission region. For the purposes of calculation, equation 5.6 may be written as a summation,

$$N_K(\text{total}) = \sum_{i=1}^N \bar{N}_{Ki} P_i \Delta z \quad (5.6)$$

This corresponds to dividing the OH emission region into  $N$

layers of thickness  $\Delta z$ . In the  $i^{\text{th}}$  layer the volume emission rate is  $P_i$  and the fraction of the effective population in the  $k^{\text{th}}$  rotational level is  $N_{ki}$ .

### 5.2.2 Numerical results.

The local effective rotational populations have been calculated for the ninth and eighth vibrational levels, for the initial population distributions described in §5.1.5, using temperatures and collision frequencies from the United States Standard Atmosphere Tables (1966), and the OH emission height profile of Packer (1961).

In all calculations, the value of  $Q_{10}$  (the probability per collision of a transition between the first and second rotational levels), is taken as unity. This means that every collision will cause a rotational transition. No relevant measurements are available for the OH molecule, but Evenson and Broida (1966) have found that in CN every collision will cause a transition.

The results of these calculations for the ninth vibrational level are given in Table 5.2 with the fractional effective populations listed every 5 km.

The total atmospheric effective populations are given in Table 5.3, expressed in terms of rotational population "temperatures" (c.f. §4.3.3). These values are those that would be determined for the rotational "temperatures" from the analysis of ( $v'=9$ ) band emission spectra for ground based observations of the OH nightglow.

TABLE 5.2

EFFECTIVE ROTATIONAL POPULATIONS OF NINTH VIBRATIONAL  
LEVEL AS A FUNCTION OF HEIGHT

Height (km.)	Rotational Quantum Number K									
	1	2	3	4	5	6	7	8	9	10
65	.246E-0	.258E-0	.209E-0	.139E-0	.795E-1	.403E-1	.206E-1	.653E-2	.185E-2	.422E-3
70	.263E-0	.266E-0	.206E-0	.131E-0	.717E-1	.357E-1	.192E-1	.537E-2	.134E-2	.259E-3
75	.276E-0	.270E-0	.200E-0	.122E-0	.672E-1	.356E-1	.225E-1	.539E-2	.115E-2	.181E-3
80	.269E-0	.257E-0	.188E-0	.118E-0	.740E-1	.477E-1	.376E-1	.739E-2	.127E-2	.154E-3
85	.202E-0	.204E-0	.168E-0	.130E-0	.109E-0	.883E-1	.820E-1	.141E-1	.212E-2	.216E-3
90	.880E-1	.110E-0	.124E-0	.136E-0	.164E-0	.164E-0	.183E-0	.280E-1	.385E-2	.341E-3
95	.165E-1	.307E-1	.538E-1	.913E-1	.152E-0	.243E-0	.357E-0	.499E-1	.529E-2	.453E-3
100	.129E-2	.440E-2	.155E-1	.388E-1	.148E-0	.233E-0	.497E-0	.554E-1	.696E-2	.323E-3
105	.315E-4	.218E-3	.127E-2	.677E-2	.343E-1	.166E-0	.739E-0	.492E-1	.263E-2	.120E-3
110	.967E-6	.128E-4	.136E-3	.131E-2	.120E-1	.105E-0	.843E-0	.379E-1	.142E-2	.461E-4
115	.292E-7	.721E-6	.139E-4	.240E-3	.394E-2	.621E-1	.906E-0	.274E-1	.706E-3	.162E-4
120	.181E-8	.724E-7	.222E-5	.615E-4	.160E-2	.403E-1	.937E-0	.209E-1	.402E-3	.705E-5
125	.161E-9	.978E-8	.451E-6	.186E-4	.728E-3	.274E-1	.955E-0	.171E-1	.272E-3	.401E-5
130	.014E-9	.132E-8	.911E-7	.564E-5	.330E-3	.185E-1	.968E-0	.129E-1	.154E-3	.174E-5

TABLE 5.3

ROTATIONAL TEMPERATURES ( $T_{ROT}$ ) OF EFFECTIVE  
EMITTING POPULATION, NINTH VIBRATIONAL LEVEL

	Rotational Quantum Number K								
	1	2	3	4	5	6	7	8	9
$T_{ROT}$ (°K)	227.3	257.1	287.8	362.7	525.1	1212.2	390.5	284.5	245.7

The eighth vibrational level is populated directly by the ozone-hydrogen reaction (§5.2.2), and by radiative transition from the ninth vibrational level. The fraction of the population of the ninth level that undergoes transitions into the eighth is given by the ratio of the radiative transition probability for the (9-8) band,  $A_{98}$ , to the sum of the probabilities for all radiative transitions from the ninth vibrational level. The number of molecules undergoing the (9-8) transition per unit time,  $N_{98}$ , is,

$$N_{98} = N_9 \frac{A_{98}}{\sum_{v''=0,8} A_{9v''}} \quad (5.7)$$

where  $N_9$  is the rate of excitation into the ninth vibrational level, and  $A_{9v''}$  is the probability for radiative transition between vibrational levels 9 and  $v''$ . Using the values for the relative transition probabilities from Stair et al. (1970), this reduces to,

$$N_{98} = 0.134 N_9 \quad (5.8)$$

If the rate of direct population of the ninth vibrational level is four times that for the eighth (Velculescu, 1970), the total rate of population of the eighth vibrational level,  $N_8$  is,

$$\begin{aligned} N_8 &= 0.250 N_9 + 0.134 N_9 \\ &= 0.384 N_9 \end{aligned} \quad (5.9)$$

Direct population, therefore, accounts for approximately 66% of the total rate of population of the eighth vibrational level,

the remainder occurring through radiative transition from the ninth level.

The initial population distribution of the eighth vibrational level is determined by the distribution of the directly excited population, and by the distribution of the population arising from the radiative transitions from the ninth vibrational level. The former population is assumed to be confined to a single rotational level (§5.1.5), and the latter is the effective emitting population of the ninth vibrational level, redistributed by transitions (c.f. §4.3).

The fractional effective populations have been calculated for the eighth vibrational level, for every 5 km, and are listed in Table 5.4. The total atmospheric effective population is given in Table 5.5, expressed in terms of rotational population "temperatures". These values would be determined as rotational "temperatures" from the analysis of ( $v'=8$ ) band emission spectra from ground based observations of the OH night-glow. The same information is shown as a rotational temperature graph in Figure 5.1. For comparison, the rotational temperature graph values from the (8-4) and (8-3) band spectra in the airglow atlas of Broadfoot and Kendall (1968) are given. The equilibrium calculations (§3.3) for the (8-4) band are also shown. It is apparent that the weak interaction relaxation model results agree well with observations, and the equilibrium model results do not. Discrepancies between the observations and the weak interaction theory can be explained by the uncertainties in the absolute radiative transition probabilities,

TABLE 5.4  
EFFECTIVE ROTATIONAL POPULATIONS OF EIGHTH VIBRATIONAL  
LEVEL AS A FUNCTION OF HEIGHT

Height (km.)	1	2	3	4	5	6	7	8	9	10
65	.240E-0	.247E-0	.196E-0	.127E-0	.707E-1	.362E-1	.191E-1	.119E-1	.915E-2	.805E-2
70	.257E-0	.255E-0	.192E-0	.118E-0	.620E-1	.309E-1	.170E-1	.116E-1	.962E-2	.881E-2
75	.269E-0	.256E-0	.183E-0	.106E-0	.539E-1	.278E-1	.171E-1	.133E-1	.119E-1	.113E-1
80	.259E-0	.237E-0	.162E-0	.920E-1	.495E-1	.301E-1	.226E-1	.199E-1	.189E-1	.186E-1
85	.184E-0	.172E-0	.126E-0	.826E-1	.554E-1	.422E-1	.363E-1	.344E-1	.342E-1	.353E-1
90	.808E-1	.876E-1	.802E-1	.693E-1	.589E-1	.512E-1	.435E-1	.416E-1	.420E-1	.483E-1
95	.216E-1	.328E-1	.450E-1	.572E-1	.645E-1	.648E-1	.480E-1	.386E-1	.249E-1	.307E-1
100	.336E-2	.940E-2	.211E-1	.440E-1	.633E-1	.863E-1	.589E-1	.521E-1	.119E-1	.719E-2
105	.128E-3	.719E-3	.330E-2	.131E-1	.438E-1	.107E-0	.629E-1	.104E-0	.122E-1	.119E-2
110	.744E-5	.804E-4	.674E-3	.481E-2	.287E-1	.122E-0	.491E-1	.132E-0	.107E-1	.570E-3
115	.413E-6	.838E-5	.129E-3	.166E-2	.177E-1	.134E-0	.356E-1	.150E-0	.838E-2	.304E-3
120	.420E-7	.139E-5	.438E-4	.692E-3	.118E-1	.141E-0	.274E-1	.160E-0	.665E-2	.183E-3
125	.568E-8	.284E-6	.104E-4	.319E-3	.814E-2	.146E-0	.223E-1	.166E-0	.564E-2	.129E-3
130	.794E-9	.581E-7	.318E-5	.146E-3	.558E-2	.149E-0	.182E-1	.170E-0	.435E-2	.759E-4



TABLE 5.5  
 ROTATIONAL TEMPERATURES ( $T_{ROT}$ ) OF EFFECTIVE  
 EMITTING POPULATION, EIGHTH VIBRATIONAL LEVEL

	Rotational Quantum Number K								
	1	2	3	4	5	6	7	8	9
$T_{ROT}$ (°K)	199.0	209.2	228.5	264.6	348.4	369.2	488.2	478.7	568.4

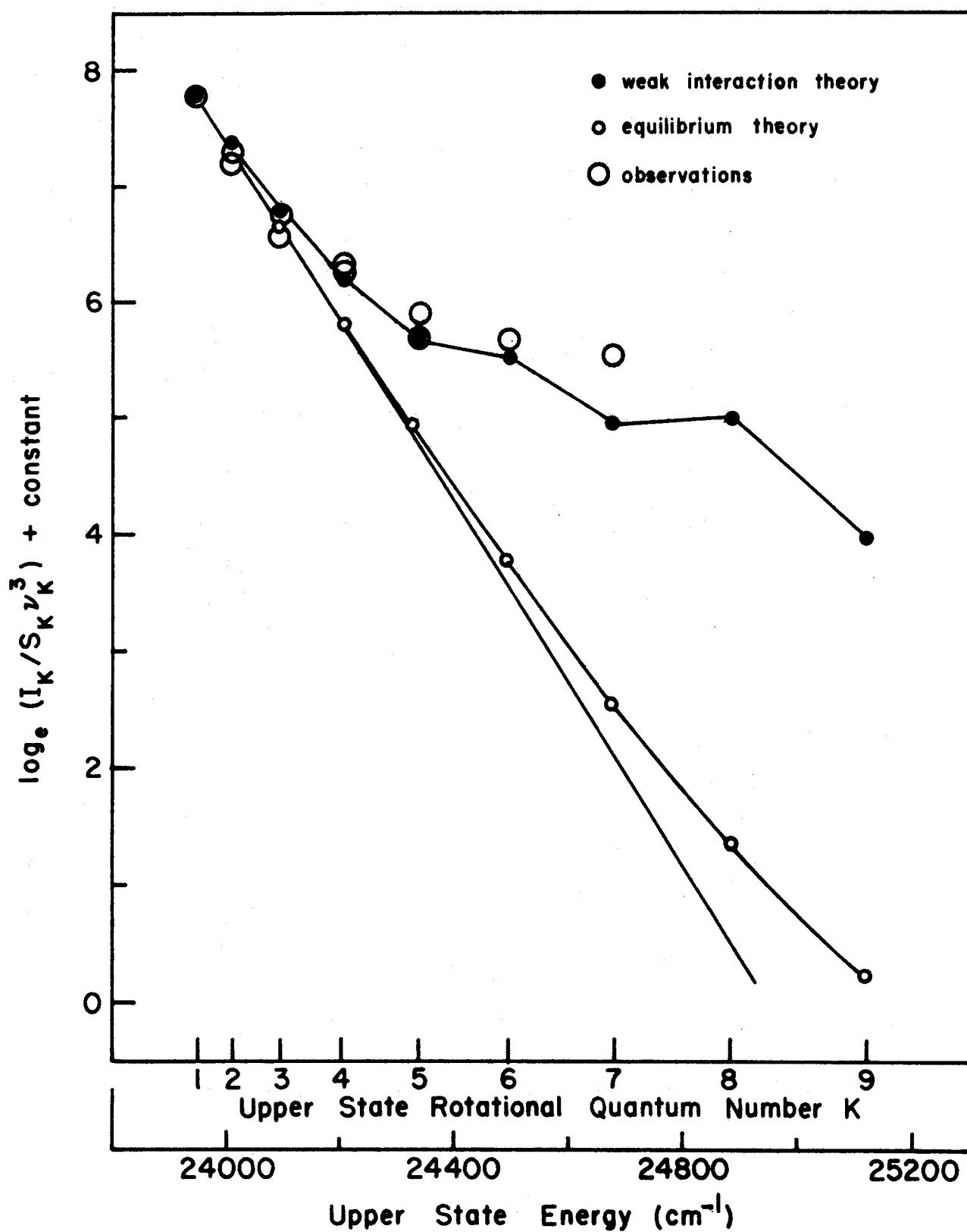


Figure 5.1: Comparison of rotational temperature graphs for theory and observations.

and the lack of accurate information on the initial populations from the excitation mechanism.

### 5.2.3 Discussion

The accuracy of these calculations is limited by two sources of error, assuming that the weak interaction theory holds rigorously. Firstly, the initial population distribution from the excitation mechanism is not known accurately. Secondly, the effective populations depend on the values of the absolute radiative transition probabilities. No accurate measurements of the absolute transition probabilities have yet been made of OH, and present estimates are based on the HCl molecule (Heaps and Herzberg, 1951). Also, vibrational relaxation has been ignored. Subsequent discussions will show that it may be important for atmospheric OH emissions.

The calculations for the eighth and ninth vibrational levels indicate the general behaviour of the corresponding OH rotational populations in the atmosphere, but due to the uncertainties, an extension of these calculations to lower vibrational levels is not justified. The behaviour of the rotational populations of the lower vibrational levels may still be described qualitatively. It is apparent from equations 4.38 and 4.40 that the value of  $B_v$  affects the rate at which the rotational population relaxes. If  $B_v$  increases, the magnitudes of the exponential terms in equation 4.40 decrease. As these exponential terms correspond to collisional transitions which increase the rotational quantum number of the excited molecule,

an increase in  $B_v$  results in a more rapid relaxation of the population. The value of  $B_v$  increases for decreasing vibrational levels (c.f. equation 4.10) and therefore the relaxation of a given rotational population will be more rapid in the lower vibrational levels.

If the lower vibrational levels are populated by radiative cascade from higher vibrational levels, the populations in the lower vibrational levels will have undergone more collisions than those in the upper vibrational levels. Therefore, the atmospheric OH spectra emitted from the lower vibrational levels will be more nearly isothermal than the spectra from the upper vibrational levels.

### 5.3 The Role of Vibrational Relaxation

#### 5.3.1 Introduction

Herman and Shuler (1958) have shown that vibrational relaxation in excited molecular species is much slower than rotational relaxation, and that the two may be considered separately for practical computation. This permits consideration of the effects of rotational relaxation in atmospheric OH molecules, independently of vibrational relaxation. However, vibrational relaxation is important in determining relative vibrational populations of OH molecules in laboratory experiments (Anlauf et al., 1968), and therefore it may affect the OH band intensities in the airglow. Although a complete discussion is beyond the scope of the present work, a qualitative consideration of the role of vibrational relaxation in OH

airglow processes is instructive.

### 5.3.2 Theory

The energy spacing between consecutive vibrational energy levels in the OH molecule electronic ground state is approximately  $3000\text{ cm}^{-1}$  ( $\sim 0.4\text{ eV}$ ) (Krassovsky *et al.*, 1962), and it follows from the discussions in §4.6 that vibrational relaxation satisfies the adiabatic requirement. Therefore, vibrational relaxation may be described accurately in terms of weak interaction theory.

Herman and Shuler (1958) have assumed that the probability for collision-induced rotational transitions is between  $10^2$  and  $10^5$  times larger than that for vibrational transitions. Findlay and Polanyi (1964) have found that collision induced vibrational transitions in HCl occur for one in every  $6 \times 10^3$  collisions. There is evidence to suggest that approximately 500 collisions are required for OH (Broida, 1962). These data indicate that the collisional efficiency for vibrational transitions,  $Q_{VIB}$ , is  $\sim 10^{-3}$ .

From the previous discussions for rotational relaxation, vibrational relaxation should not substantially affect the emitted spectrum unless the time between collision-induced vibrational transitions is equal to, or shorter than, the radiative lifetime. The condition for vibrational relaxation to be important may be written in terms of the collision frequency,  $\nu$ , the collisional efficiency,  $Q_{VIB}$ , and the radiative transition probability,  $A_V$ ,

$$A_V < \nu Q_{VIB} \quad (5.10)$$

Substitution into this equation of the presently assumed values for  $A_V$ ,  $Q_{VIB}$  and  $\nu$  indicates that vibrational relaxation will be important in OH airglow emissions below  $\sim 75$  km. Thus, it will be particularly important in the dayglow and twilight emissions of OH, due to the substantial fraction of the emission below 75 km. (Llewellyn and Evans, 1971).

### 5.3.3 Temperature dependence and band intensities

The temperature dependence of rotational relaxation was discussed in §4.5.3. It was shown that the rotational population required more collisions with increasing temperature to reach equilibrium. The temperature dependence of rotational relaxation is determined by the weak interaction process. Vibrational relaxation is also a weak interaction process, and will therefore have the same temperature dependence as rotational relaxation.

Radiative decay and collisional de-excitation compete in the deactivation of vibrational level populations, and thus an increase in the rate of vibrational relaxation will cause a decrease in the intensity of vibration-rotation band emissions. An increase in the rate of relaxation will result from a decrease in kinetic temperature, or an increase in collision frequency. Changes in either temperature, or collision frequency, will therefore be reflected by changes in the intensity of the emitted bands.

#### 5.3.4 Comparison with observations

These theoretical predictions may be compared with the observed behaviour of the OH nightglow. The relevant observations are those published by the Russian workers, which give correlations between the intensities and rotational temperatures and other phenomena.

The only information on the ambient temperatures from these observations is the rotational temperature measurements. These "temperatures" were derived assuming an isothermal behaviour in the emitting molecules. To evaluate this information, it is necessary to consider the effect of attributing a single emission temperature to spectra from non-equilibrium populations. It is equivalent to fitting a straight line to the rotational temperature graphs (e.g. Figure 3.4). The less the effective population has relaxed, the higher is the temperature derived from the slope of the straight line of best fit. Applied to the Russian data, this means that high "isothermal rotational temperatures" will correspond to little relaxation in the effective population. "Temperature" determined in this manner does not correspond to a kinetic temperature. The isothermal rotational temperature is a parameter which can be used to describe the degree of relaxation in the effective rotational population. It should be noted that all "rotational temperatures" reported by Russian authors have been determined in this manner. The observational results indicate that in general the isothermal rotational temperature is highest for bands from the ninth vibrational level, and decreases with

decreasing vibrational quantum number . This shows that the rotational relaxation is least for the highest vibrational levels -- in agreement with the predictions of the weak interaction theory.

Due to the temperature dependence of the rotational relaxation process (§4.5.3), an increase in ambient temperature will reduce the degree of relaxation of the effective population, and therefore cause an increase in the isothermal rotational temperature. Therefore, changes in the ambient kinetic temperature will cause changes in the same sense in the isothermal rotational temperature. Changes in the isothermal rotational temperature do not necessarily indicate changes in the ambient kinetic temperature, as the rotational relaxation is also affected by changes in the collision frequency and the collisional efficiency.

With this information, it is possible to explain some of the features of the intensity and "temperature" variations in the OH nightglow. The atmospheric temperature profile varies with season: in the region of the OH emissions the ambient temperature is highest in winter. At an altitude of 85 km, at latitude 60°, the temperature difference between summer and winter is 51°K (United States Standard Atmosphere, 1966). Therefore, both the vibrational and rotational relaxation rates will be lowest in winter. This means that the OH vibration-rotation bands will be most intense in winter, and the highest isothermal rotational temperatures will be obtained from spectra recorded in winter. These results agree exactly with observations



(Shefov and Truttse, 1969).

Another feature of the OH airglow variations that can be explained by the rotational and vibrational relaxation processes is the correlation of intensity and isothermal rotational temperature. It has been observed that for the vibration-rotation bands from the higher vibrational levels ( $v' \geq 6$ ), variations in intensity show a good correlation with variations in isothermal rotational temperature (Krassovsky, 1963). This behaviour may be understood by considering the effects of a change in the ambient kinetic temperature. If the temperature increases, both vibrational and rotational relaxation rates will be reduced. This will cause an increase in band emission intensities and a simultaneous increase in the isothermal rotational temperature. Similarly, a decrease in ambient temperature will cause a simultaneous decrease in band intensities and isothermal rotational temperature. The predicted behaviour agrees with the observational evidence for the upper vibrational levels. The correlation between intensity and isothermal rotational temperature has recently been observed for the lower vibrational levels ( $v' \leq 5$ ), (Harrison *et al.*, 1971) and does not support the conclusion of additional excitation mechanisms for the OH molecule into these levels (Breig, 1970; Shefov and Truttse, 1969).

It is clear from the above discussions that weak interaction vibrational and rotational relaxation processes are capable of explaining qualitatively a number of observed features of the OH airglow emissions. Although this lends support to

the suggestion that rotational relaxation is a weak interaction process, it does not prove it. However, it does indicate that if rotational relaxation is a strong interaction process, it must have the same temperature dependence as the weak interaction process.

## CHAPTER VI

### SUMMARY AND CONCLUSIONS

#### 6.1 The Present Work

The analysis of observations of nightglow spectra has shown that for the OH (4-1) and (5-2) bands the rotational intensity distribution cannot be explained in terms of emission from excited molecules in rotational equilibrium at a single temperature. This result has been confirmed by analysis of OH spectra from the nightglow spectrum atlas of Broadfoot and Kendall (1968).

It has been found that emissions from OH molecules, in rotational equilibrium with the ambient atmosphere, will exhibit non-isothermal rotational temperatures due to the variation in kinetic temperature throughout the airglow emitting region. The deviation from isothermal behaviour introduced in this manner is in the same sense as that for the observed results, but is too small to explain the observations. Other effects which could contribute to the observed non-isothermal behaviour have also been considered. It has been shown that the assumption of rotational equilibrium for the excited molecules is incorrect and that non-equilibrium processes are important in determining the OH nightglow spectrum.

The effects of non-equilibrium processes on the emitted spectrum have been considered for assumed initial vibration-rotation level populations and for different thermalization processes. In general a given excited vibrational level may

be populated by radiative transition from a higher level, or directly from the excitation mechanism. It has been found that the rotational population distribution is changed by radiative transitions so that the population distribution in the lower state is different from that in the upper state.

The thermalization of the excited molecular state rotational population may be described by a relaxation process. A simple classical model has been considered which can be used to describe the relaxation of Boltzmann rotational population distributions. The discrete nature of the rotational energy levels has prevented the application of this model to the relaxation of OH molecules.

To permit an analysis of rotational relaxation for molecules with discrete rotational energy levels, a theory similar to that of Herman and Shuler (1958) has been proposed. In this theory, a weak interaction between kinetic and rotational energies is assumed, and collisions cause rotational transitions which are allowed by the optical transition selection rules. To determine the emitted spectrum for a collisionally relaxing population, the theory has been extended to include radiative decay.

The derived radiative relaxation equation has been applied to the atmospheric OH emissions to calculate the vibration-rotation spectrum that should be observed. As the collision frequency and the kinetic temperature are functions of height in the atmosphere, and both affect the rate of collisional relaxation, the emitted spectrum is different

at different heights. The ground observed spectrum has been determined from the summation of these individual height spectra over the total region of emission.

To permit the calculation of these spectra it has been necessary to estimate the probable vibrational level populations originating in the excitation mechanism. It has been assumed that the only mechanism for the excitation of the OH nightglow emissions is the reaction between atomic hydrogen and ozone. Laboratory experiments (Anlauf et al., 1968) suggest that this reaction will populate the eighth and ninth vibrational levels with total energies close to the heat of reaction.

The total radiating rotational populations have been calculated for the eighth and ninth vibrational levels. The calculated rotational temperatures for the eighth vibrational level are in good agreement with rotational temperatures calculated from observations of the (8-4) and (8-3) OH bands reported by Broadfoot and Kendall (1968). The discrepancies have been attributed to uncertainties in the values of the absolute radiative transition probabilities, lack of accurate knowledge of the levels populated by the excitation mechanism, and the effects of noise in the observed spectra. From qualitative considerations it has been shown that for a given collision frequency and temperature, the effective rotational populations are more relaxed in the lower vibrational levels than in the upper.

It has been assumed that the vibrational and

rotational energy modes relax independently so that the rotational population distribution is not affected by vibrational relaxation. However, it has been suggested that vibrational relaxation may influence the relative intensities of the vibration-rotation bands in the airglow. It has been shown that vibrational relaxation is described by a weak interaction process, and that the collisional efficiency for vibrational de-excitation is  $\sim 0.1\%$  of that for rotational de-excitation. Therefore, vibrational relaxation should be important for OH emissions originating at altitudes below 75km.

It has been shown that the proposed relaxation theory is able to explain a number of observed features in the OH nightglow spectrum. The quantitative agreement between the observed and calculated deviations from isothermal behaviour is excellent for the analysed bands. In addition, the extent of rotational relaxation expected for the different vibrational levels is in the same sense as that for the observed spectra (Krassovsky, 1963). The temperature dependence of this relaxation theory also provides a qualitative explanation of the seasonal behaviour of the OH emission intensities and isothermal rotational temperatures, and for the correlation between variations in these quantities.

## 6.2 Suggestions for Future Work

### 6.2.1 OH emissions

The present investigation has shown the importance of relaxation processes for the atmospheric OH emissions. The accuracy of this work has been limited by the uncertainty of

the absolute radiative transition probabilities, and the vibrational and rotational population distributions from the excitation mechanism. When these quantities are better known, it will be valuable to extend the rotational relaxation calculations to the lower vibrational levels for a detailed comparison of the theory with experimental data.

The absolute radiative transition probabilities can be determined from an accurate measurement of the electric dipole moment of the OH molecule. Estimates of these transition probabilities may also be obtained from rotational relaxation measurements in laboratory spectra, but the accuracy will depend on the reliability of the value used for the collisional efficiency for rotational de-excitation, and on the assumption that rotational relaxation is a weak interaction process. The collisional efficiency depends on the collision cross section for rotational transitions of the OH molecule, which may be estimated from the collision broadening of the OH( $^2\Pi$ ) spectral lines. A comparison of the values of the absolute radiative transition probabilities determined by these two methods should provide some indication of the validity of a weak interaction process to describe rotational relaxation.

The effects of vibrational relaxation in laboratory experiments to study the OH excitation mechanism should be eliminated if the results are to be applied to calculations for the atmosphere. It is possible that the vibrational de-excitation conditions are different in the atmosphere, as the collision partners for the relaxing OH molecules are

different in the two situations: in the atmosphere the OH molecules will collide principally with  $N_2$  and  $O_2$  molecules, while in the laboratory ozone-hydrogen reaction, the collisions will be with  $O_3$ , OH, and H.

To determine the behaviour of vibrational relaxation in the atmosphere, laboratory ozone-hydrogen reactions should be investigated in the presence of excess  $N_2$  and  $O_2$ , at very low pressures ( $<10^{-4}$  torr). If the production of molecules such as  $NO_2$  and  $H_2O$  is small\*, the same experiments should give practical information on airglow rotational relaxation.

When the role of vibrational relaxation is known, a comparison of laboratory data with the atmospheric OH emissions should provide an indication of the relative importance of secondary excitation mechanisms for the OH airglow.

#### 6.2.2 Application to other emissions

The relaxation calculations which have been considered in this work may also be applied to non-equilibrium processes for other molecules. Cashion and Polanyi (1960) have observed a deviation from isothermal behaviour in rotational temperatures derived from the vibration-rotation bands of HCl, obtained in the laboratory from the reaction between H and  $Cl_2$ . They attribute the non-isothermal behaviour to the initial excitation mechanism.

It may be difficult to determine the initial vibrational

---

\*These molecules are known to be efficient at rotational deactivation of OH molecules, and if present in any amount, could affect the results.



and rotational population distributions arising from the excitation mechanism, as evidence suggests that all of the heat of reaction does not always go into the newly formed band (Findlay and Polanyi, 1964). It is also uncertain if weak interaction theory applies to the HCl molecule, due to the spacing between the rotational energy levels ( $\sim 20 \text{ cm}^{-1}$ ).

Relaxation processes may also be important in the emission spectrum of  $\text{OH}(^2\Sigma^+)$  in acetylene flames. The observed rotational temperatures deviate considerably from isothermal behaviour (Ticktin *et al.*, 1967; Broida, 1955). It is probable that self absorption contributes to observed deviations (Broida, 1955), and that background emissions are important (Dieke and Crosswhite, 1948). Therefore, the contribution from non-equilibrium processes may be difficult to determine. It is also possible that the rotational relaxation in  $\text{OH}(^2\Sigma^+)$  may involve strong interactions between kinetic and rotational energy, as collision induced transitions have been observed that violate the weak interaction theory selection rules (Carrington, 1959).

Deviation from isothermal behaviour has been observed in the rotational temperatures determined from the  $\text{N}_2^+$  First Negative bands in aurora (Harrison, 1955; Montalbetti, 1957). It has been shown that the population distribution of excited molecules is determined by the equilibrium population in ground state  $\text{N}_2$  molecules (Hunten, 1961). The  $\text{N}_2^+$  First Negative bands arise from allowed transitions so that rotational temperatures determined using the  $B_v$  value for ground state  $\text{N}_2$  should

correspond to the kinetic temperature. The observed deviations from isothermal behaviour in the rotational temperatures should arise from the atmospheric profile weighting effect discussed for OH. This should permit rocket observations of the  $N_2^+$  First Negative band spectra to provide accurate atmospheric temperature profiles throughout the emission region.

Relaxation calculations should apply to the auroral emission from the  $N_2$  Vegard-Kaplan bands. These emissions originate from the magnetic dipole transition  $A^3\Sigma_u^+ - X^1\Sigma_g^+$  at a height of approximately 200 km (Hunten and McElroy, 1966). The radiative lifetime of the ( $^3\Sigma_u^+$ ) level is uncertain but has been estimated as between 1 second and 15 seconds (Ahmed, 1969). At a height of 200 km, the collision frequency is  $\sim 3 \text{ sec}^{-1}$  so that radiating molecules experience between 3 and 45 collisions per radiative lifetime. Rotational relaxation in molecular nitrogen does not obey weak interaction theory, and experimental evidence indicates that 3 to 10 collisions are required to cause thermalization (Herman and Shuler, 1958). Therefore, the Vegard-Kaplan emissions may originate from molecules that are only partially thermalized.

It has been concluded previously that the emissions originate from a thermalized rotational population (Ahmed, 1969), but the method used in determining the rotational temperatures was insensitive to deviations from isothermal behaviour. To clarify the role of relaxation processes in the  $N_2$  Vegard-Kaplan emissions, spectra of higher resolution are necessary. The results from such spectra should give information on strong

interaction rotational relaxation mechanisms.

It is concluded that the application of relaxation calculations to the emission spectra of atmospheric molecules may provide an important tool in the understanding of the processes in the upper atmosphere.

---

# REFERENCES

- Ahmed, M. 1969 J. Atmos. Terr. Phys. 31, 1259.
- Anlauf, K.G.,  
MacDonald, R.G., and  
Polanyi, J.C. 1968 Chem. Phys. Lett. 1, 619.
- Baker, D.J. and  
Waddoups, R.O. 1967 J. Geophys. Res. 72, 4881.
- Bates, D.R. and  
Nicolet, M. 1950 C. Rendus Acad. Sci. Paris 230,  
1943.
- Bauer, H.J.,  
Kneser, H.O. and  
Sittig, E. 1959 J. Chem. Phys. 30, 1119.
- Benedict, W.S.,  
Plyler, E.K. and  
Humphreys, C.J. 1953 J. Chem. Phys. 21, 398.
- Blackwell, D.E.,  
Ingham, M.F. and  
Rundle, H.N. 1960 Astrophys. J. 131, 15.
- Breig, E.L. 1970 Planet. Space Sci. 18, 1271.
- Broadfoot, A.L. and  
Kendall, K. 1968 J. Geophys. Res. 73, 426.
- Broida, H.P. 1955 Temperature, its Measurement  
and Control in Science and  
Industry. Vol. 2, p. 265.  
Reinhold Publishing Co., N.Y.
- Broida, H.P. 1962 J. Chem. Phys. 36, 444.
- Brout, R. 1954 J. Chem. Phys. 22, 934.
- Carrington, T. 1959 J. Chem. Phys. 31, 1418.
- Cashion, J.K. and  
Polanyi, J.C. 1960 Proc. Roy. Soc. Lond. A258, 529.
- Cashion, J.K. 1963 J. Mol. Spec. 10, 182.
- Chamberlain, J.W., and  
Smith, C.A. 1959 J. Geophys. Res. 64, 611.
- Chamberlain, J.W. 1961 Physics of the Aurora and  
Airglow, p. 490. Academic  
Press, New York.

- |  |      |  |
|--|------|--|
| Clarke, J.F. and<br>McChesney, M.                        | 1964 | <u>The Dynamics of Real Gases</u> ,<br>Butterworths, London.             |
| Dieke, G.H. and<br>Crosswhite, H.M.                      | 1948 | "Bumblebee Series" Report No.<br>87. Johns Hopkins University.           |
| Evans, W.F.J.,<br>Wood, H.C., and<br>Llewellyn, E.J.     | 1970 | Can. J. Phys. <u>48</u> , 747.   |
| Evenson, K.M. and<br>Broida, H.P.                        | 1966 | J. Chem. Phys. <u>44</u> , 1637.   |
| Findlay, F.D. and<br>Polanyi, J.C.                       | 1964 | Can. J. Chem. <u>42</u> , 2176.  |
| Harrison, A.W.   | 1955 | M.Sc. Thesis, University of<br>Saskatchewan.                             |
| Harrison, A.W.   | 1970 | Can. J. Phys. <u>48</u> , 2231.  |
| Harrison, A.W.,<br>Llewellyn, E.J. and<br>Nicholls, D.C. | 1970 | Can. J. Phys. <u>48</u> , 1766.  |
| Harrison, A.W.,<br>Evans, W.F.J. and<br>Llewellyn, E.J.  | 1971 | To be published.   |
| Heaps, H.S. and<br>Herzberg, G.                          | 1962 | Z. Physik <u>133</u> , 48.   |
| Heppner, J.P. and<br>Meredith, L.H.                      | 1958 | J. Geophys. Res. <u>63</u> , 51.   |
| Herman, R.C. and<br>Hornbeck, G.A.                       | 1953 | Astrophys. J. <u>118</u> , 214.  |
| Herman, R. and<br>Wallis, R.F.                           | 1955 | J. Chem. Phys. <u>23</u> , 637.  |
| Herman, R. and<br>Shuler, K.                             | 1958 | J. Chem. Phys. <u>29</u> , 366.  |
| Herzberg, G.   | 1950 | <u>Spectra of Diatomic Molecules</u> ,<br>D. van Nostrand Co., New York. |
| Hill, E.L. and<br>Van Vleck, J.H.                        | 1928 | Phys. Rev. <u>32</u> , 250.  |
| Hönl, H. and<br>London, F.                               | 1925 | Z. Physik <u>33</u> , 803.   |

- |  |      |   |
|--|------|---|
| Hund, F.   | 1927 | Z. Physik <u>42</u> , 93.   |
| Hunten, D.M.   | 1961 | Ann. Geophys. <u>17</u> , 249.  |
| Hunten, D.M. and<br>McElroy, M.B.                    | 1966 | Rev. Geophys. <u>4</u> , 303.   |
| Kaufman, F.  | 1964 | Ann. Geophys. <u>20</u> , 106.  |
| Kozlov, V.P.   | 1966 | Izvestia Atmospheric and<br>Oceanic Physics <u>2</u> , 80.  |
| Krassovsky, V.I.,<br>Shefov, N.N. and<br>Yarin, V.I. | 1962 | Planet. Space Sci. <u>9</u> , 883.  |
| Krassovsky, V.I.                                     | 1963 | Planet. Space Sci. <u>10</u> , 7.   |
| Krassovsky, V.I. and<br>Shefov, N.N.                 | 1965 | Space Sci. Rev. <u>4</u> , 176.   |
| Kvifte, G.   | 1959 | J. Atmos. Terr. Phys. <u>16</u> ,<br>252.   |
| Llewellyn, E.J. and<br>Evans, W.F.J.                 | 1971 | <u>The Radiating Atmosphere</u> ,<br>Ed. Billy M. McCormac.<br>Reidel Publishing Co, Holland<br>(in press). |
| Lowe, R.P.   | 1960 | C.A.R.D.E. tech. memo #291/59<br>Valcartier, Quebec.  |
| Meinel, A.B.   | 1950 | Astrophys. J. <u>111</u> , 555.   |
| McPherson, D.H. and<br>Vallance Jones, A.            | 1960 | J. Atmos. Terr. Phys. <u>17</u> , 302.  |
| Montalbetti, R.                                      | 1957 | Can. J. Phys. <u>35</u> , 831.  |
| Norrish, R.G.W.                                      | 1964 | Inst. Intern. Chim. Solvay,<br>Conseil Chim. <u>12</u> , 99.  |
| Nicolet, M.  | 1970 | Ann. Geophys. <u>26</u> , 531.  |
| Phelps, D.H. and<br>Dalby, F.W.                      | 1965 | Can. J. Phys. <u>43</u> , 144.  |
| Packer, D.M.   | 1961 | Ann. Geophys. <u>17</u> , 67.   |
| Polanyi, J.C.  | 1959 | J. Chem. Phys. <u>31</u> , 1338.  |
| Raff, L.M. and<br>Winter, T.G.                       | 1968 | J. Chem. Phys. <u>48</u> , 3992.  |

- |  |      |  |
|--|------|--|
| Reed, E.I. and<br>Blamont, J.E.  | 1967 | Space Research VII, Vol. 1,<br>p. 337.   |
| Shefov, N.N.   | 1961 | Spectral, Electrophotometric<br>and Radar Studies of the Polar<br>Aurora and Nightglow. No. 5<br>p. 5.       |
| Shefov, N.N. and<br>Truttse, Y.L.  | 1969 | Annals of IQSY <u>4</u> , 400.   |
| Shuler, K.E.   | 1959 | Phys. Fluids <u>2</u> , 442.   |
| Stair, A.T.,<br>Huppi, E.R.,<br>Sanford, B.P.,<br>Murphy, R.E.,<br>O'Neil, R.R.,<br>Hart, A.M.,<br>Huppi, R.J.,<br>Pendelton, W.R. | 1971 | <u>The Radiating Atmosphere</u> ,<br>Ed. Billy M. McCormac.<br>Reidel Publishing Co., Holland<br>(in press). |
| Takayanagi, K.   | 1952 | Progr. Theoret. Phys. (Japan)<br><u>8</u> , 497.   |
| Tarasova, T.M.   | 1961 | Ast. Circ. Acad. Sci. U.S.S.R.<br>#222, p.31.  |
| Ticktin, S.<br>Spindler, G. and<br>Schiff, H.I.  | 1967 | Disc. Farad. Soc. <u>44</u> , 218.   |
| Twomey, S.   | 1965 | J. Franklin Inst. <u>279</u> , 95.   |
| United States Standard<br>Atmosphere Supplements   | 1966 | United States Government<br>Printing Office, Washington.   |
| Velculescu, V.G.   | 1970 | Z. Physik <u>237</u> , 69.   |
| Wallace, L.  | 1961 | J. Atmos. Terr. Phys. <u>20</u> , 85.  |
| Wallace, L.  | 1962 | J. Atmos. Sci. <u>19</u> , 1.  |
| Wilkes, M.V.   | 1966 | <u>A Short Guide to Numerical<br/>Analysis</u> , Cambridge University<br>Press.                              |